Water Colour and Temperature in the Southern Beaufort Sea: Remote Sensing in Support of Ecological Studies of the Bowhead Whale

G.A. Borstad

Western Region
Department of Fisheries and Oceans
Winnipeg, Manitoba R3T 2N6

June 1985

Canadian Technical Report of Fisheries and Aquatic Sciences No. 1350

Canadian Technical Report of Fisheries and Aquatic Sciences

Technical reports contain scientific and technical information that contributes to existing knowledge but which is not normally appropriate for primary literature. Technical reports are directed primarily toward a worldwide audience and have an international distribution. No restriction is placed on subject matter and the series reflects the broad interests and policies of the Department of Fisheries and Oceans, namely, fisheries and aquatic sciences.

Technical reports may be cited as full publications. The correct citation appears above the abstract of each report. Each report is abstracted in *Aquatic Sciences and Fisheries Abstracts* and indexed in the Department's annual index to scientific and technical publications.

Numbers 1–456 in this series were issued as Technical Reports of the Fisheries Research Board of Canada. Numbers 457–714 were issued as Department of the Environment, Fisheries and Marine Service, Research and Development Directorate Technical Reports. Numbers 715–924 were issued as Department of Fisheries and the Environment, Fisheries and Marine Service Technical Reports. The current series name was changed with report number 925.

Technical reports are produced regionally but are numbered nationally. Requests for individual reports will be filled by the issuing establishment listed on the front cover and title page. Out-of-stock reports will be supplied for a fee by commercial agents.

Rapport technique canadien des sciences halieutiques et aquatiques

Les rapports techniques contiennent des renseignements scientifiques et techniques qui constituent une contribution aux connaissances actuelles, mais qui ne sont pas normalement appropriés pour la publication dans un journal scientifique. Les rapports techniques sont destinés essentiellement à un public international et ils sont distribués à cet échelon. Il n'y a aucune restriction quant au sujet; de fait, la série reflète la vaste gamme des intérêts et des politiques du ministère des Pêches et des Océans, c'est-à-dire les sciences halieutiques et aquatiques.

Les rapports techniques peuvent être cités comme des publications complètes. Le titre exact paraît au-dessus du résumé de chaque rapport. Les rapports techniques sont résumés dans la revue *Résumés des sciences aquatiques et halieutiques*, et ils sont classés dans l'index annual des publications scientifiques et techniques du Ministère.

Les numéros 1 à 456 de cette série ont été publiés à titre de rapports techniques de l'Office des recherches sur les pêcheries du Canada. Les numéros 457 à 714 sont parus à titre de rapports techniques de la Direction générale de la recherche et du développement, Service des pêches et de la mer, ministère de l'Environnement. Les numéros 715 à 924 ont été publiés à titre de rapports techniques du Service des pêches et de la mer, ministère des Pêches et de l'Environnement. Le nom actuel de la série a été établi lors de la parution du numéro 925.

Les rapports techniques sont produits à l'échelon régional, mais numérotés à l'échelon national. Les demandes de rapports seront satisfaites par l'établissement auteur dont le nom figure sur la couverture et la page du titre. Les rapports épuisés seront fournis contre rétribution par des agents commerciaux.

Canadian Technical Report of

Fisheries and Aquatic Sciences 1350

June 1985

WATER COLOUR AND TEMPERATURE IN THE SOUTHERN BEAUFORT SEA: REMOTE SENSING IN SUPPORT OF ECOLOGICAL STUDIES OF THE BOWHEAD WHALE

by

G. A. Borstad[1]

Western Region

Department of Fisheries and Oceans

Winnipeg, Manitoba R3T 2N6

This is the 181st Technical Report

from the Western Region, Winnipeg

---

[1] G.A. Borstad Limited, 10474 Resthaven Drive, Sidney, B.C. V8L 3H7

PREFACE

This is the final report of work conducted under the terms of a Department of Supply and Services contract awarded as a result of an Unsolicited Proposal (DSS Contract No. 06SB.FP941-3-1335). The scientific authority was Dr. J.F.R. Gower, Remote Sensing, Institute of Ocean Sciences, 9860 West Saanich Road, Sidney, British Columbia, V8L 4B2. This report is published upon recommendation by Mr. R. Peet, Freshwater Institute, Department of Fisheries and Oceans, Western Region, Winnipeg.

Cat. No. Fs 97-6/1350E ISSN 0706-6457

Correct citation for this publication is:

Borstad, G.A. 1985. Water colour and temperature in the southern Beaufort Sea: remote sensing in support of ecological studies of the bowhead whale. Can. Tech. Rep. Fish. Aquat. Sci. 1350: v + 68 p.

TABLE OF CONTENTS

LIST OF FIGURES

LIST OF PLATES

LIST OF APPENDICES

ABSTRACT

Borstad, G.A. 1985. Water colour and temperature in the southern Beaufort Sea: remote sensing in support of ecological studies of the bowhead whales. Can. Tech. Rep. Fish. Aquat. Sci. 1350: v + 68 p.

Comparison of the geographic distribution of bowhead whales in the southern Beaufort Sea and coincident observations of water colour, chlorophyll a fluorescence and/or temperature made from aircraft and satellites during August-September 1980-1983, show that important congregations of bowheads (and many smaller groupings also) tend to occur in the vicinity of oceanographic phenomena manifesting themselves as surface temperature or turbidity fronts and anomalies. This is in agreement with suggestions that bowheads feed in areas of local zooplankton abundance, since zooplankton are known to often accumulate at discontinuties and upwellings. It may be possible to use satellite imagery to predict bowhead distribution.

Key words: bowhead whales; Beaufort Sea; water colour; chlorophyll a fluorescence; surface water temperature; airborne remote sensing; satellite imagery.

RESUME

Borstad, G.A. 1985. Water colour and temperature in the southern Beaufort Sea: remote sensing in support of ecological studies of the bowhead whales. Can. Tech. Rep. Fish. Aquat. Sci. 1350: v + 68 p.

Une comparaison effectuée entre les données de la répartition géographique des baleines boréales dans les régions du sud de la mer de Beaufort et les observations coïncidentes de la couleur de l'eau, de la température et (ou) de la fluorescence de la chlorophylle a à partir d'un aéronef ou d'un satellite, entre les mois d'août et septembre des années 1980 à 1983, montre que les baleines boréales se réunissent en groupes importants ou en petits groupes surtout près de phénomènes océanographiques prenant la forme d'écarts prononcés de température à la surface et d'anomalies et de fronts de turbidité. Cette constatation corrorobore les hypothèses selon lesquelles les baleines boréales se nourrissent dans les régions où abonde le zooplancton, puisque celui-ci s'accumule de toute évidence dans les discontinuités et les résurgences marines. Il pourrait être possible d'utiliser à l'avenir les photographies spatiales pour prédire la répartition de baleines boréales.

Mots-clés: baleines boréales; mer de Beaufort; couleur de l'eau; fluorescence de la chlorophylle a; température de l'eau superficielle; détection aérienne; photographie spatiale.

INTRODUCTION

The bowhead whale Balaena mysticetus is a large baleen whale previously abundant in cold Arctic waters. Commercial whaling during the last century drastically reduced the population to about 3-4000 animals in the Western Arctic and somewhat smaller number in the Eastern Arctic (International Whaling Commission 1983). It is now considered an endangered species by the International Whaling commission and under American legislation. The largest remaining population winters in the Bering Sea and summers in the Canadian Beaufort, migrating around Alaska and through the Chukchi Sea in spring and fall (Braham et al. 1980; Ljungblad et al. 1982). During the spring migration the animals are far offshore, but during their exit from the Beaufort many bowheads pass through or near the zones of oil exploration off the Mackenzie River delta and along the Alaskan north coast (Ljungblad et al. 1982; Richardson et al. 1983).

Large-scale, comprehensive aerial surveys of bowhead whale distribution have now been conducted off both the Alaskan and Canadian coasts for several years, partly in an attempt to determine whether or not the industrial activity in having a detectable effect on the distribution or behaviour of the whales. These studies have shown that the distribution or behaviour of the animals is highly variable from year to year in the southeast Beaufort Sea off the Yukon Coast and Tuktoyaktuk Peninsula (Richardson 1983). Even in the presence of disturbance by man's activities, it is reasonable to expect the distribution and movements of the population to be affected by its physical environment and food supply. There is evidence that bowheads tend to be found at locations having significantly higher zooplankton biomass (Griffiths and Buchanan 1982); however, there are almost no data concerning zooplankton distribution in the Beaufort Sea. Because of the logistical problems and the cost of such a study there has not yet been an attempt to relate bowhead whale distribution to food abundance over a large area, or to physical factors which at least partly determine the distribution of zooplankton.

The present study represents an application of relatively recent technology to the problem. Coincident with the 1983 bowhead whale surveys which were carried out by LGL Ltd. (McLaren and Davis 1984) for the Environmental Studies Revolving Fund (DIAND) and managed by Dome Petroleum Limited, we employed airborne remote sensing techniques developed by Gower and Borstad (Neville and Gower 1977; Gower and Borstad 1981; Borstad and Brown 1980; Borstad et al. 1981; Borstad and Gower, in press) to map water colour patterns in the southern Beaufort Sea. Sea surface temperature was also measured from the aircraft using a PRT-5 radiometer, but an instrument fault made the data unretrievable. Temperature patterns present during the 1983 surveys were determined from coincident satellite imagery. The water colour and temperature data were compared to the 1983 bowhead distributions reported by McLaren and Davis (1984), and a small number of satellite thermal images from 1980, 1981 and 1982 were also compared to bowhead distributions in those years summarized by Richardson (1983).

Our airborne measurements were made from the whale survey aircraft using the Institute of Ocean Sciences colour spectrometer. While such water colour surveys have been conducted in the Arctic before (Borstad and Gower, in press), the 1983 surveys were carried out in an opportunistic mode, that is the flight lines, altitude and times were chosen to suit the whale observations. We tried to impose as little disruption as possible to normal survey routines. Within these limitations, the objectives of the project were to:

1. Obtain presently lacking descriptive data concerning the distribution and patterns of phytoplankton crops (chlorophyll concentration) in the Southern Beaufort Sea during the period of maximum open water (August);
2. Provide preliminary assessment of the relationship between the primary producers and the physical forces or processes governing their growth and distribution (by comparison of chlorophyll and temperature data); and
3. Acquire data concerning the importance of frontal zones and circulation patterns on the productivity of the region;
4. Compare the distribution of bowhead whales to the temperature and water colour fields on large and small scales, and seek to answer the question as to whether or not the distribution of feeding whales is related to measurable physical (temperature) or biological (chlorophyll concentration, sediment) variation or discontinuities.

The study also included an investigation of available satellite imagery with more limited objectives to: compare the ice, temperature and water colour patterns visible in NOAA - AVHRR imagery for the month of August, 1979 to 1983. Where imagery is available for the time of a whale survey, compare bowhead distribution to observed oceanographic structure. Attempt to obtain Coastal Zone Colour Scanner Imagery for the Beaufort Sea for the period August - September, 1983.

BACKGROUND ON METHODOLOGY

REMOTE WATER COLOUR MEASUREMENT

The amount of visible radiation emerging from the sea (the upwelling signal) is determined by the absorption and scattering characteristics of the upper layers of the water column, by the downwelling radiation incident upon the sea surface and by the transmission characteristics of the surface itself. Within the water the spectral character of the incident radiation is altered by absorption of water and by dissolved and suspended material including planktonic algae. The backscatter from particulate matter is essentially white, however the strong spectal nature of the absorption by water, phytoplankton and dissolved organic material (summarized in Figure 1) result in the change of apparent and measurable colour of water bodies with increasing chlorophyll a (+ phaeopigments) content. Since water itself

absorbs strongly at longer wavelengths, radiant energy emerging from plankton-poor water will be mostly blue. Increasing phytoplankton chlorophyll a concentrations result in decreases in the amount of blue upwelling light (because of strong absorbance by chlorophyll a and phaeopigment at these wavelengths) and a progressive greening of the water (Morel 1980). For remote sensing purposes, chlorophyll a and the phaeopigments are generally summed, since their absorption properties are similar.

Remote measurements of the chlorophyll content of a water body have generally made use of these changes in the amounts of blue (440 nm) and green (560 nm) upwelling radiance ($L_u(\lambda)$) after normalizing them to the amount and spectral nature of the downwelling incident irradiance ($E_d(\lambda)$) (Clarke et al. 1970; Curran 1972; Arvesen et al. 1973; Miller et al. 1976; Morel 1980 and others). Examples of the resulting reflectance spectra $L_u\lambda/E_d$ or $R_L(\lambda)$ in Figure 2 illustrate the changes associated with increases in pigment concentration. (The reflectance as calculated here and by others for remote above-water measurements is a mixed radiance-irradiance ratio which differs from subsurface irradiance ratios by π/Q - 0.6 because of Fresnel reflection and refraction which occurs as the upwelling signal leaves the water (Austin 1980; Morel 1980).) Experiments show that there is a direct relation between the ratio of the green reflectances around 550 nm and those at blue wavelengths (440 nm is usually chosen) and pigment concentration in the top 5-10 m of the water column. There are, however, a number of factors interfering with this measurements, which will be discussed later. For this work we have chosen to use a pair of wavelengths much closer together (550 nm and 525 nm) which is less sensitive to other influences.

We also employ a second independent method for remote detection and measurement of chlorophyll a based on in vivo fluorescence by the pigment. This phenomenon has been exploited for experimental and measurement purposes for many years and oceanographers have made use of the in vivo fluorescence by phytoplankton chlorophyll a to infer continuous chlorophyll vertical or horizontal distribution using filter fluorometers. These instruments generally use weak 0.2 $\mu W/cm^2$ blue light (maximum near 440 nm) to excite the pigment while recording all emissions greater than 650 nm (Yentsch and Menzel 1963; Lorenzen 1967).

Naturally stimulated in vivo fluorescence by the chlorophyll a molecule was first detected on reflectance spectra by Neville and Gower (1977) as a distinct gaussian peak of 35 nm half power band width centered at 684 nm. Figure 2 illustrates the increases of Fluorescence Line Height (FLH) that are associated with increasing chlorophyll a concentration. Because of the very strong red absorption by water, the observable fluorescence signal will be confined to the uppermost 1-2 m of the water column. The weak attenuation of long wavelengths in the atmosphere does not grossly affect the upwelling fluorescence signal which exits the water, and FLH may even be measurable at spacecraft altitudes (Gower and Borstad 1981).

The two methods are in a sense more complementary than similar. For both measurements the reflectance signal (R_L at 525 and 550 nm, and around 685 nm) represents an optically weighted average of the upper layer of water and its contents. Since the absorption by water at short wavelengths is much less than at red lengths the effective penetration depth for G/B and FLH will be different. For British Columbia waters we have empirically found that G/B measures chlorophyll a in the uppermost 5-10 m layer, while FLH measures the pigment concentration of a layer only 1-2 m thick. Generally, the factors interfering with the chlorophyll measurement by G/B (surface reflection, atmospheric reflectance, dissolved organic material) do not grossly affect FLH, however physiological variability of in vivo fluorescences may affect this index.

Where inorganic particulate material (riverine sediments or glacial flour) is present, it can dominate the optical processes and alter or mask the chlorophyll signal at low pigment concentrations. Since the backscatter and absorption spectra of sediment are generally white, we utilize wavelengths at which interference by other colourants such as chlorophyll are minimum. We have used a measure of red reflectance at 640 nm and a ratio of green to red reflectance (at 550 nm and 640 nm) as indices of total suspended material (Johnson and Munday 1983); at shorter wavelengths absorption by phytoplankton and reflection from the sea surface can interfere, while at longer wavelengths absorption by atmospheric water vapour can be a problem.

REMOTE TEMPERATURE MEASUREMENT

Remote temperature measurement, whether from spacecraft or aircraft is carried out with radiometers sensitive to infra-red radiation in the 10-12 μm region of the electromagnetic spectrum. This wave band is usually chosen because absorption by the atmosphere, water vapour, maritime aerosols and stratospheric aerosols is minimized there. Because of the very strong absorption of these wavelengths by liquid water, radiometers viewing a water surface measure the temperature of a very thin surface skin (top 0.1 mm). The skin temperature may differ by a few tenths of a degree from the water temperature a few centimetres below, where conventional sea surface temperature is usually measured. The presence of a diurnal thermocline in the top metre will also result in discrepancies between the remote (skin) and in situ temperature measurement. This effect will be greatest during clear, calm afternoons in protected lakes and bays, or where a shallow freshwater lens is present on the sea.

The best multi-band atmospheric corrections for stallite data are accurate to about 0.5°C (Robinson et al. 1984) although simple empirical field calibration of the raw data to the same accuracy is possible for limited areas provided sufficient in situ temperatures are available within a few hours of the image (Tabata and Gower 1980). Single channel airborne radiometers can usually be calibrated to

within 0.5C° also and when measurements are made at low altitude, atmospheric effects are reduced. Even light fog, mist or rain can cause large errors, however.

INSTRUMENTATION AND METHODOLOGY

AIRBORNE WATER COLOUR MEASUREMENTS

The Institute of Ocean Sciences spectrometer

The Institute of Ocean Sciences (I.O.S.) spectrometer (described in detail by Walker et al. 1974, 1975) employs a 256 channel silicon diode array as its sensing element. The diode array measures light focussed by a 35 mm focal length f/2 Nikon camera lens onto a 100 µm wide slit, which is in turn in the focal plane of a 35 mm focal length f/2 Erfle eyepiece. Collimated light from this lens is reflected from a 300 line per millimetre reflection grating blazed at 760 nm and refocussed by the same lens in a Littow arrangement back onto the diode array in such a way as to register the spectral range of 380 to 1035 nm.

A simplified diagram of the spectrometer system as used in 1983 is illustrated in Figure 3. For this project the optical sensing unit was mounted on the floor of the aircraft so that it looked horizontally at a front surface mirror which directed the optical path either up through a tube at an opal glass diffuser mounted on top of the aircraft, or down at a second mirror through a polarizing filter and out at the sea. The upper optical path allowed spectral measurements of the incident signal (sun + sky irradiance). The lower path viewed the sea surface at an angle of 53° from the vertical (the Brewster Angle), and could be rotated to any azimuth so as to allow the operator to look away from sun glitter. The purpose of the polarizing filter in the lower (upwelling) light path was to block light reflected from the sea surface, which at the Brewster Angle is almost completely polarized. This arrangement is particularly important for operations under cloud where the reflected signal is very high.

The diode array can be scanned in approximately 0.1 second with a variable frequency of 8, 4, 2 or $1 \cdot s^{-1}$. The integrated output from each diode is digitized and recorded on computer compatible tape using a custom-built microcomputer. After each scan the diodes are re-zeroed and where several seconds of data are averaged, the signal-to-noise ratio is approximately 2000:1. The custom-designed data acquisition system also can record up to 16 analog channels of asociated information at 12 bit accuracy. For this project, much of the data was collected under extreme conditions of low sun angle and low signal strength. Except for some flights made over open pack, data were summed over from 1, 2 or 4 seconds (shorter over bright turbid water; longer over dark, clear water). Since the acceptance angle of the spectrometer is relatively small (0.17 x 0.7°), the instantaneous footprint on the sea surface from 150 m altitude was about 1.4 x 6 m. However, this was smeared by the forward velocity of the aircraft (about 50 $m \cdot s^{-1}$), so that the survey data are for areas between 50 and 200 m along the flight path.

The I.O.S. spectrometer and data acquisition package as used for this project weighed approximately 160 kg and required 28 V power at 15 amps. The electronics components were configured in 2 short racks shock-mounted in two fibreglass shipping crates of dimensions 60 x 70 x 80 cm. The optical "head" was attached to the data acquisition system by a 5 m cable. The 1983 configuration of the optical periscope made use of two holes in the aircraft fuselage: one of 5 cm diameter in the upper skin, and a second of approximately 15 cm diameter in the lower skin.

Airborne radiation thermometer (Barnes PRT-5)

The Barnes PRT-5 instrument is a commercially available radiometer which measures naturally emitted radiation in the 9.5 to 11.5 µm range by continually comparing it ot the energy emittted by an internal temperature controlled reference enclosure. Incoming radiation is interrupted at a frequency of 100 Hz by a highly reflective optical chopper thus enabling the detector to view the sea and the temperature reference alternately. The detector itself is an immersed thermistor which converts the energy received into a voltage directly related to the temperature difference of the sea and the reference. The field of view of the instrument is 2° which at 150 m altitude means that the instantaneous footprint on the sea surface is 5 m in diameter. The I.O.S. instrumentation package includes a PRT-5 which is capable of measuring sea surface temperature to ±0.5°C in the laboratory and to about 1°C under normal field conditions.

Unfortunately, an intermittent short in the PRT-5 recorder output connector through which data were routed caused the temperature data for the 1983 surveys to be recorded with a varying baseline. Because the real-time strip-chart recorder was not operated (Section 3.1.6) this problem was not recognized in the field. We consider the data unreliable and have not analysed them.

Aircraft

The aircraft used for this project was a de Havilland Twin Otter, rented from Kenn Borek Air, Inuvik, by Dome Petroleum Limited for the whale surveys. All flights were made at an altitude of 150 m and an airspeed of 180 km/h according to normal survey procedures (McLaren and Davis 1984). The aircraft was equipped with an automatic pilot, global navigation system and radar altimeter.

Personnel

The whale survey required a pilot and two observers. Since navigation was not our responsibility, only one person (Dr. G. Borstad or Dr. J. Gower) accompanied the instrumentation on the first few flights. This person operated the data acquisition system and monitored the equipment. He also kept a log of spectrometer operations and features visible on the sea, such as lines of flotsam, colour changes, sea state,

internal waves and ice as well as notes concerning sky condition and cloud cover.

After 21 August, an Arctic Laboratories technician (B. Clegg) was also on most flights, in order to train in the operation of the instrumentation. On some flights, S. Lin, an oceanographer from the People's Republic of China or B. Smiley (DFO) flew as observers.

Observing conditions

Flight lines and scheduling were determined by the requirements of the whale survey. Most flights left Tuktoyaktuk shortly after 0800 MDT, with survey lines beginning as early as 0830 MDT (0530 local solar time). Since the visual whale survey was not severly affected by ambient light conditions many flights were made under heavy overcast with very low incident levels. The water colour measurements made under these conditions were very noisy and some data were unusable for this reason.

Haze and mist were encountered over a large fraction (30-40%) of the survey area in both August and September. While corrections for light mist are partly successful, about 20% of the water colour data are unrecoverable. Impenetrable fog covered about 5% of the survey line kilometres in August and 20% in September, mostly over the warmer riverine plume. Open pack ice occupied most of the western-most line in September with a tongue extending east along the Yukon Coast and across Mackenzie Bay just offshore of the river plume.

Equipment performance

The I.O.S. equipment was shipped to Inuvik during the week prior to the first survey and tested on 15 August. Test data sent to Victoria for processing did not detect any problems and the equipment was installed in a Kenn Borek Ltd. aircraft on 18 August. The initial installation took four hours. The aircraft and water colour crew flew to Tuktoyaktuk on the 19 and began the first survey at 0930 MDT that morning.

Normally, the I.O.S. instrumentation provides two channels of uncalibrated data in real time (usually the PRT-5 record and either G/B or FLH) as a continuous stripchart. During the first hour of the survey flight on the 19th the data were observed to be extremely noisy. The skies were very heavily overcast and the extremely low signals were partly responsible. However, since ground loops between instruments were suspected, the AC inverters and the AC pen recorder were turned off, and the PRT-5 was disconnected from the spectrometer data acquisition system. Later tests in the air and on the ground failed to locate the problem and the inverters and recorder were left off-line. Noise was noted during later flights but it appeared to be much less and nothing more was done during the August survey. When the digital data were processed the noise was about 10x normal levels.

Before the September survey, the aluminum tube used for the incident signal was electrically insulated from the aircraft skin and a heavy ground cable was attacted between the spectrometer optical head and the data acquisition system rack. This reduced the electrical noise to normal levels. The PRT-5 was reconnected, but the AC inverters and stripchart were left off-line.

Calibration of airborne reflectance data

Joint aircraft/helicopter exercises: In order to calibrate the reflectance data for conditions similar to those encountered during the surveys, three calibration exercises were carried out: on 21 August near the edge of the turbid river plume off Pullen Island; on 23 August in a line from 70°30'N south to Tuktoyaktuk; and on 9 October in the Eskimo Lakes and Liverpool Bay. In these exercises, airborne reflectance measurements were made simultaneously with collection of surface water samples at a total of 39 stations. All these reflectance data were collected from 150 m altitude except at 10 stations where reflectance data were also measured from 300 m altitude in order to obtain an estimate of the path radiance contributed by the atmosphere below the aircraft (see DATA PROCESSING section). The latitude and longitude of the calibration stations was obtained from global navigation systems on both the aircraft and helicopter. The location of the calibration stations, place names used in the text and bottom topography are illustrated in Figure 32.

Our sampling was conducted from a single engine Bell 206 helicopter. However in future, we would strongly recommend use of a twin engine machine for safety reasons.

Collection of water samples: Because a ship was not available vertical profiles were impossible. Water samples were obtained from a helicopter hovering at 10 - 20 m altitude, by lowering a line to which two 1-L plastic bottles were attached. In situ data or samples for surface temperature, salinity, the weight of total suspended particulate material, chlorophyll a/phaeopigment concentration and phytoplankton generic compositon were collected at most stations. Secchi transparency and Munsell colour observations were obtained at most stations on 21 and 23 August. Data for all three exercises are tabulated in Appendix 3.

Temperature and salinity: Sea surface temperature was measured by inserting an AES sea temperature thermometer (0.1°C markings) into one of the 1-L water samples immediately after they were brought into the helicopter. Surface salinity of 100-mL subsamples was later measured using a Guildline Autosal.

Chlorophyll a/phaeopigment: One hundred fifty mL subsamples for pigment analysis were filtered immediately after return to shore through 2.4 cm Whatman GF/C glass fibre filters using vacuum pressure less than 150 mm mercury. A few drops of $MgCO_3$ suspension were added as the final 20 mL were filtered, and the filter blotted dry, folded and stored at -10°C. During transport from Tuktoyaktuk to Victoria the temperature of the filters came to ambient, however.

The chlorophyll a concentration in acetone extracts of the filtered phytoplankton material

was later measured by the fluorescence technique, using a G.K. Turner Model III fluorometer equipped with a R446 red-sensitive photomultiplier and blue lamp. Analysis techniques were as outlined by Strickland and Parsons (1972).

Total suspended particulate material: Subsamples of either 100 mL (21 August samples), or 200 mL (23 August) were filtered through tared 47 mm diameter 0.40µm pore Nuclepore filters within five hours of sampling. For the 9 October samples a filter manifold was available and 510-815 mL volumes were filtered during the next day. Filters were stored in plastic Petri dishes, then dried for 24 hours in a drying oven before reweighing using a Sartorius 2423 balance (d=0.01 mg).

Because the tare weights of the 21 and 23 August filters were lost in the laboratory, the weight of the suspended material contained on these filters was determined in reverse - by weighing the filter after cleaning in a sonic bath. To test the validity of this approach, Mackenzie River water containing suspended sediment was filtered through 0.4 µm Nuclepore tared filters to give loads ranging from 0 to 13 mg. After drying, each filter was separately placed in a Rapidographe ultrasonic cleaner (Model 3069 USCZ) containing deionized distilled water for 15 minutes. After replacing the water with fresh deionized distilled water each filter was then sonified for another minute. The filter was then removed from the bath using Teflon forceps, removing excess water by dragging it across the edge of a cleaned filter dish. The filters were then dried to constant weight for 24 hours in a drying oven before weighing. Results from this experiment (Appendix 5) show over-recovery at low weights and under-recovery at high weights. Almost all of the variation shown was within the weighing error ($\pm$ 0.12 mg, SD = 0.8%, n=15), which was $\pm$ 0.6 mg$\cdot$L^{-1} for the 23 August samples and $\pm$ 0.14 to 0.24 mg$\cdot$L^{-1} for the 9 October samples. The 21 August samples were not used because the reflectance data obtained on that day were badly contaminated by atmospheric water vapour and cloud.

Phytoplankton generic composition: One hundred fifty mL subsamples for identification of phytoplankton were preserved with Lugol's Iodine and stored in brown glass bottles. Because phytoplankton chlorophyll was not a major determinant of water colour at the calibration stations, these samples have not been examined.

Secchi transparency and Munsell colour: On the 21 and 23 August calibration exercises, Secchi transparency was measured by lowering a Secchi disc from the hovering helicopter. If the helicopter was above about 15 m altitude, the downwash from the rotor did not interfere with the visibility of the disc. The colour of the water layer above the disc was also subjectively measured by comparing the apparent colour of the Secchi disc at half its disappearance depth with a series of Munsell colour swatches after the method of Austin (1980).

Mapping the airborne data

During processing, stripcharts of the various indices were plotted against time. By knowing the time and positon at the start and end of each trasect, the indices could be transferred to a 1:1 000 000 scale chart with an accuracy of about 4-5 km along track. Data were continuous along the flight lines as shown by the solid lines in the distribution maps (Figures 24, 25). The isopleths were subjectively drawn by hand.

SATELLITE DATA

Providing useful data in the Beaufort

Four satellite sensors provide data relevant to this project. LANDSAT 4 and 5 both carry a multispectral scanner (MSS) and a Thematic Mapper (TM). The MSS has four 100 nm wide bands in the visible range having a spatial resolution of 80 m. The placement of band 2 (600-700 nm) makes it useful for quantitative determination of sediment concentrations greater than about 2 mg$\cdot$L^{-1}; however, the combination of the relatively low gains and wide band widths make the other bands of little use for the determination of water colour in clear waters. The TM has a spatial resolution of only 30 m. The combination of narrower bands and their placement in the blue and green part of the spectrum may allow chlorophyll mapping. Both TM also have a sensor operating in the 10.4 - 12.5 µm thermal infrared region. At the time of writing the TM on LANDSAT 4 is no longer operational. LANDSAT 5 was launched 1 March 1984.

The NOAA satellites (7 and 8) carry the Advanced Very High Resolution Radiometer (AVHRR) which has one broad band visual sensor (580-680 nm) and two infrared detectors, operating in the 10.5-12.5 thermal region. The visual sensor was designed to provide cloud and land data for use with the thermal sensor; however, it is sufficiently sensitive to be useful for sediment concentrations above about 2 mg$\cdot$L^{-1}. The thermal sensor can also provide considerable information in the Beaufort in late summer because a relatively large thermal contrast exists between the warm waters of the Mackenzie River and coastal embayments and the cold meltwater near the offshore ice pack.

The Coastal Zone Colour Scanner (CZCS) on NIMBUS-7 is an experimental multispectral scanner with five narrow band (20 nm), high gain sensors optimally placed to measure water colour. After appropriate corrections to remove atmospheric signal (which in some bands can contribute as much as 90% of the recorded signal) data from the green and blue bands can be used to calculate a chlorophyll index useful in clear waters not containing inorganic sediment. It should also be capable of mapping sediment variations under certain conditons. A sixth band has provided intermittent, rather poor quality thermal data since launch in October, 1978. At the time of writing the CZCS was not functional and the prospects for future operation look poor.

Data availability

The LANDSAT satellites are operational satellites, with an established distribution

system for the data in Canada through the Canada Centre for Remote Sensing (CCRS), but its orbit is such that for high latitudes such as the Beaufort Sea any particular area is only imaged on two or three consecutive days, every 16 days. This decreases its usefulness for describing dynamic oceanographic features. LANDSAT-4 band 2 imagery from two passes over the Yukon coast on 19 and 22 August are discussed in the description of 1983 Water Colour and Temperature Patterns section of the RESULTS AND DISCUSSION. A considerable amount of historical LANDSAT data (since 1972) is achieved at CCRS.

The AVHRR operates continuously providing 1 km resolution data with a repeat cycle of about 12 h. Since two saellites are currently operational, data for any particular area are theoretically available every 6 h. However, not all orbits are within direct acquisition range of receiving stations and without special arrangements beforehand, only one or two images per week are available. This number is further reduced by cloud. In Canada, AVHRR data are received at the CCRS Prince Albert Receiving Station (Prince Albert, Saskatchewan) and at the Atmospheric Environment Service (AES) receiving station in Edmonton, Alberta. Due to manpower constraints at AES, however, digital data have nor been available from this station since April 1983. A new receiving facility at the University of British Columbia began operation in late 1983. Digital data for the Beaufort were available from CCRS for about four days out of five during 1983. Data from previous years were obtained from the Environment Data Service in Washington, D.C. However, only a small proportion of these data are in digital form.

NIMBUS-7 operates in a polar orbit with several daily overpasses at high latitudes. On-board power limitations and demand for data elsewhere, combined with the frequent cloudiness has limited past CZCS coverage of the Beaufort Sea to one scene in August, 1980. In 1982 and 1983 this sensor was turned on only on request. In 1983, requests for imagery over the Beaufort Sea resulted in acquisition of data in this area nearly two days out of five during July, August and September. At the time of writing this 1983 imagery is not yet available because of delays in archival and processing at NASA. This data is archived at the Satellite Services Division, Environmental Data Information Service, NOAA, Washington, D.C.

DATA PROCESSING

AIRBORNE WATER COLOUR DATA

Details of correction and calibration procedures

The data processing stream for the several separate measurements required to produce a reflectance spectrum is shown in Figure 4. In all cases a reflectance measurement consists of an upwelling signal which is used in conjunction with a downwelling signal and an electrical dark signal measured less frequently. The first two signals are corrected for the spectral transmission character of the uplooking and downlooking pathways (see Equation 1 and description to follow), and the downwelling signals are updated to the time of the upwelling measurement. This updating is necessary because the instrument is a single array device.

$$R_L = \frac{U(t_2,\lambda) - D(t_2,\lambda)}{I(t_2,\lambda) - D(t_2,\lambda)} \cdot K(\lambda) \qquad \textbf{Equation 1}$$

where $U(t_2,\lambda)$ = uncalibrated spectral radiance measurement of upwelling light, uncorrected for transmission of front surface mirror or periscope glass

$I(t_2,\lambda)$ = uncalibrated spectral irradiance measurement of the downwelling (incident) signal, updated to time of upwelling measurement but uncorrected for transmission of the uplooking neutral density filter or opal glass diffuser

$D(t_2,\lambda)$ = electrical dark spectrum updated to time of upwelling measurement

$K(\lambda)$ = corrections for differences in spectral transmission of uplooking or downlooking optical pathways

t_0,t_1,t_2 = time of measurement (t_0=dark; t_1=incident; t_2=upwelling)

λ = indicates spectral measurement (380-1100 nm)

The electrical dark current spectrum (D) is recorded at intervals throughout the flight, and since it varies with the array temperature, D is updated according to changes of the signal from the last diode on the array S(380 nm) for both incident and upwelling measurements. This diode at 380 nm receives very little light from the target except a small amount which is scattered inside the instrument, because of the transmission character of the optics and sensitivity of the instrument at these wavelengths.

$$D(t_n,\lambda) = D(t_0,\lambda) - D(t_n,380\text{ nm}) \qquad \textbf{Equation 2}$$

This correction which is independent of wavelength, compensates for the internal scattering as well as the temperature dependence of the array.

The corrected dark current spectrum $D(t_2,\lambda)$, the upwelling spectrum $U(t_2,\lambda)$ and the corrected incident spectrum $I(t_2,\lambda)$ are smoothed over four adjacent diodes (approximately 12 nm). Since the spectrometer optics cause light of any given wavelength to be imaged over four diodes, this smoothing reduces the noise level without any further loss in useful information.

The incident spectrum utilized in the calculation of $I(t_1,\lambda)$ is also updated to the time of the upwelling measurement t_2 by utilizing a continuously recording single uplooking diode (C) mounted on the top of the aircraft. This diode is under an opal glass diffuser and a blue cutoff filter transmitting less than 590 nm. $I(t_2,\lambda)$ is modified according to a factor Ct_2/Ct_1 which describes the change in the intensity of the incident signal seen by the uplooking diode between t_1 and t_2.

$$I(t_2,\lambda) = I(t_1,\lambda) \times \frac{Ct_2}{Ct_1} \qquad \textbf{Equation 3}$$

This updating algorithm is based on the assumption that the spectral quality of the incident irradiance shows little variation. This is not strictly true, although tests have shown that cloud cover sufficiently strong to reduce the incident signal by a factor 10 resulted in less than 20% increase in the ratio of radiation intensity between 400 and 685 nm. Generally, variations are less than this and where large changes in incident signal are encountered, this measurement is made more often. Many of the gaps in survey data shown in the distribution maps presented in Section 5 are where the upwelling measurements were interrupted in order to obtain a new incident spectrum.

Contaminating signals

Simply put, the upwelling signal arriving at the aircraft can be thought of as the sum of three components: the water leaving radiance $L_W(\lambda)$ multiplied by the transmittance of the atmosphere $T(\lambda)$; specularly reflected radiance from the sea surface $L_G(\lambda)$; and the atmospheric path radiance $L_P(\lambda)$.

$$L = L_W(\lambda) \cdot T(\lambda) + L_G(\lambda) + L_P(\lambda) \qquad \textbf{Equation 4}$$

Most of the surface reflection $L_G(\lambda)$ is blocked by our use of a polarizer. $L_P(\lambda)$ the path radiance, is reduced simply by flying at low altitudes, but a noticeable effect can remain. Since the Rayleigh scattering component of the path radiance is predictable (following a $\lambda^{-4.09}$ law), a constant correction scaled to the aircraft altitude should be successful at correcting for most of the effects of gaseous components in the atmosphere. However, the effect of the atmospheric aerosols (suspended particulates or liquids) is not strictly predictable and should be measured. Aerosol scattering is also assumed to follow a λ^{-n} power law; however, n the Angstrom coefficient varies with the type and size of aerosols. Since many marine aerosols increase in size due to deliquesence as relative humidity increases, they form a haze which can reduce visibility by scattering light. The vertical and horizontal distribution of aerosols can vary considerably (Wallace and Hobbs 1977; Gordon and Clarke 1980; Sturm 1981).

Tests made during earlier projects showed that for the very clear days on which we generally chose to fly, and for the altitudes at which we operated, the combined atmospheric effects were small and relatively constant over wide areas. Under these circumstances we could make reflectance measurements for a target from two different altitudes and calculate the reflectance contribution by the atmospheric layer between them by subtraction. This atmospheric reflection signal was pro-rated according to the survey altitude and subtracted from survey data to arrive at sea surface reflectances. For this project, however, we were not able to wait for optimal atmospheric conditions because we were hitchhiking on the whale survey aircraft. We were also not able to make frequent measurements of the atmospheric effects, since this would have required repeated overflights at differing altitudes and added to the time required for the surveys. We did make these measurements as part of the calibration exercises carried out 21 and 23 August and 9 October and have subtracted a mean atmospheric signal proportional to the survey altitude from the water spectra. This assumption of uniformity may lead to increasing errors as atmospheric turbidity increases.

Because time in the field did not allow for a very thorough investigation of these effects in this area, we have empirically reduced errors in the G/B due to this factor in three ways. First, we utilized a ratio of two wavelengths relatively close together, placed so as to be sensitive to water colour variations but not severely affected by atmospheric contamination. Second, we monitored the absolute upwelling radiance at 780 nm, where for non-turbid waters at least, the radiance should be very nearly zero. For areas away from the very turbid plume water, the G/B was adjusted according to a linear relationship between G/B and R_{780nm} derived from data obtained on 8 September when the aircraft flew over an isolated patch of mist on the outer portion of line 0. Where R_{780} became greater than about 3% because of mist or fog, the water data were considered unretrievable. Finally, we have plotted the G/B data at relatively wide contour intervals. We are confident most of the error due to atmospheric effects is contained within these error limits.

Scattering is not the only atmospheric effect. In areas where large changes are occurring in the atmosphere over short distances (such as near weather fronts), absorption by water vapour and oxygen can show up as spectral differences between incident and upwelling measurements made more than a few kilometres apart. This absorption then appears on the reflectance data as negative peaks which by their location interfere with our usual FLH calculation (Figure 5). If the shape of the absorption were constant, it would be possible to correct the reflectance spectra by adding a similar (but positive) shaped signal sufficient to fill the 760 nm oxygen absorption feature. In practice this is not possible because the relative depths of the lines vary. This problem could be reduced by making more frequent spectral incident measurements (every few minutes) but this would complicate the field routine and lengthen the time required for data processing. Redesigning the system to look alternately up at the sky and down at the sea, or adding a second optical unit to continuously monitor the spectral nature of the incident signal would be preferable solution.

For the 1983 survey data, where chlorophyll concentrations and the observed FLH were low, these atmospheric absorption effects (in part caused by our current incident updating scheme) were sometimes severe enough to preclude using FLH as an index of chlorophyll. The areas affectd are marked on the distribution maps for both August and September.

Comparison of remotely acquired data with surface samples

The 21 August calibration exercise was confined to a relatively small area, and within

a few kilometres of a weather front and fog bank. Many of the water colour spectra are contaminated by water vapour and oxygen absorption (Figure 5) and cannot be used for calibration. However, good water colour data were obtained on August 23, (Figure 6). This was a relatively clear day and the exercise took place within a few hours of solar noon and over a large area, thus covering a wide range of water types (station locations are shown on the distribution maps (Figure 15, 16) and in Figure 32. A third exercise was attempted several times in September but difficulties in scheduling the aircraft, a twin-engine helicopter, open water and good weather delayed it until 9 October. Since most of the study zone was covered by open pack by that time, the exercise was carried out in the Eskimo Lakes and Liverpool Bay. The sun elevation was extremely low, but skies were clear and no atmospheric absorption problems were encountered (Figure 7).

Chlorophyll a/phaeopigment concentration: Only a very narrow range of chlorophyll a concentrations (0.01-0.66 mg chlorophyll a $\cdot m^{-3}$) was encountered during the three calibration exercises. Where the Fluorescence Line Height (FLH) observed during the survey was equal to or less than that observed for the calibration stations having suspended particulate material (SPM) less than 2 $mg \cdot L^{-1}$, a surface concentration of less than 1 mg chlorophyll $\cdot m^{-3}$ has been inferred.

Absolute calibration of higher FLH is not possible because calibrations made in British Columbia waters have all been carried out in sediment-free waters. Where concentration of inorganic particles were present above about 2 $mg \cdot L^{-1}$, their increased backscatter increased the overall reflectance and otherwise modified the spectral character of the water, giving anomalously high FLH. A rough estimate of the pigment concentrations near Herschel Island, based on the shape, size and placement of the 550 nm peak and the height of the FLH peak at 685 nm relative to the green peak suggests levels in the range of 2-5 mg chlorophyll a $\cdot m^{-3}$. This estimate is not confirmed by in situ measurements.

The green blue ratio (G/B) is not extensively used as an index of chlorophyll a concentration, especially with data from the Coastal Zone Colour Scanner (e.g., Gordon and Clarke 1980). This is only possible where phytoplankton dominate the absorption and scattering processes. During the time of our surveys the chlorophyll concentrations over much of the Beaufort were very low and most of the blue-green colour variations were probably caused by variations of the SPM content. Because chlorophyll concentration roughly covaried with SPM at most calibration stations (Figure 8), the G/B ratio appears to provide an index of both chlorophyll a + phaeopigment (C+P) and SPM (Figure 9A, B). This covariance, however, probably did not occur everywhere in the study area. For instance the G/B and sediment indices (R640 and G/R discussed in the next section) disagreed in the area north of the Mackenzie River Delta. Because of the possible interference between chlorophyll and SPM, and because we suspect that dissolved organic materials from the river may also have been affecting the G/B, we have not used it as an index. The lack of in situ vertical profiles in all types of water mass encountered limits our ability to calibrate the G/B data.

Suspended particulate material: Figure 10 illustrates the relationship between the weight of surface suspended particulate material (SPM) and two indices (a) the reflectance at 640 nm (R 640); and (b) a ratio of the reflectance at 560 and 660 nm (G/R). The relationship between R 640 nm and Secchi transparency is shown in Figure 11. In spite of the fact that the 9 October data were collected much later in the season when the sun elevation was much less, the data agree reasonably well. The better agreement with the green/red ratio (G/R) than with R 640 probably reflects the fact that a ratio further removes between-station variations in downwelling irradiance. For the relatively good conditions under which the 23 August and 9 October calibrations were done, the G/R ratio was a more accurate index of total suspended material than was the red reflectance, R 640. The G/R ratio was much more susceptible to interference by mist and haze, however, and the sediment maps discussed in RESULTS AND DISCUSSION utilize both indices. The accuracy of the quantitative estimate of total suspended material is therefore about ± 1 $mg \cdot L^{-1}$ at low concentration and ± 2 $mg \cdot L^{-1}$ above about 10 $mg \cdot L^{-1}$. The dashed 1 mg $\cdot L^{-1}$ isopleth in the August suspended particulate map (Figure 16) reflects an uncertainty north of the Delta caused by contours apparently following the flight lines made on different days. Since this interval is at the limit of our calibration no attempt has been made to resolve this difficulty. Agreement in other areas was better, usually because R 640 dropped to very near zero offshore.

SATELLITE DATA

NOAA series AVHRR thermal imagery

In order to determine the dates and times of suitable cloud-free imagery over our study area, data from the AVHRR band (visible band 1) were first obtained from CCRS in protographic print form for several days in August and September, 1983. Digital data for cloud-free days over the Beaufort were then obtained from either the Prince Albert Receiving Station or the Satellite Services Division, Environmental Data Information Service (EDIS), Suitland, Maryland. Digital data were also obtained from EDIS to coincide with past whale surveys (1980, 1981, 1982). Since not all thermal data are archived in digital form at EDIS, some of these data are in the form of photographic prints of both the thermal and visual bands.

Processing of the digital data was carried out on the Institute of Ocean Sciences Image Processor. The images were geometrically rectified to an equal-area projection; a digitized coastline was applied; and the visible data were used to mask land, cloud and ice features in the image. The visual display of the thermal signal was also adjusted so as to optimally portray the range of values from the water areas (contrast stretching). No atmospheric corrections have been applied, for as Tabata and Gower (1980)

have demonstrated the brightness temperatures measured at the spacecraft are linear with sea surface temperatures with a fairly constant offset. This is demonstrated in Figure 12 which illustrates a comparison of the raw band 4 digital counts for the 22 August 1983 thermal image (Plate 3) with sea surface temperatures measured one day before and one day after the image. The difference in the y-intercept between the two days can be ascribed to variations in atmospheric absorption. We would choose a line midway between the two regressions as representative of the central part of the 22 August image, but because of variations of atmospheric signal across the scene, the absolute calibration may vary. The digital data were not received until early March and the time available did not allow presentation of the images in Plates 2 to 9 (including that for 22 August) in calibrated form. For the same reason we have not attempted to find historical data with which to describe the subsurface structure of features shown in the images. Nevertheless, the imagery very dramatically demonstrates the surface thermal patterns present. Both temperature and turbidity are depicted as increasing from blue to red. Note that similar colour in two images do not imply similar temperatures or turbidity.

Comparison of bowhead whale distribution with temperature patterns required that the whale positions be digitized and plotted on the imagery. The accuracy of these positions is limited by the accuracy to which they were plotted in the reports we used as sources and by the accuracy of our digitization. Overall accuracy should be better than 5 km along 1983 transects (McLaren and Davis 1984), and better than 10 km for the historical distribution summarized by Richardson (1983). The latter authors did not show each location, but used symbols of varying size to simplify their maps.

The AVHRR data obtained in print format have not been presented here for two reasons: (1) they were of such poor quality that the thermal structure was barely visible; and (2) they were returned to EDIS for reprocessing and were received only two days before the end of the project.

NOAA series AVHRR visible imagery

The most important use of AVHRR band 1 (0.58-0.68 nm) for oceanic remote sensing is usually as an indication of cloud which will contaminate the thermal signal. In the Beaufort, however, the upwelling radiance from the bright Mackenzie River plume is well within the dynamic range of the AVHRR band 1. A simple comparison of the 22 August 1983 band 1 digital counts with the weights of suspended particulate material collected on 21 and 23 August, illustrates this potential. It is perhaps surprising that the agreement is this good, considering the water movements and atmospheric changes possible in 48 h. None of the visible images in Plates 2 to 9 have been calibrated, but Figure 13 shows that the brightness in band 1 is a linear function of suspended material, at least over the range 2-20 $mg \cdot L^{-1}$.

LANDSAT-4 MSS imagery

The MSS band 2 prints (Plate 1) and the false colour transparencies were examined and a sketch map was drawn from each image to illustrate the interpretation. No geometric correction was required for these purposes.

NIMBUS-7 CZCS imagery

The CZCS data for 20 August 1980 were obtained from EDIS via Dr. Phil Hill, Atlantic Geoscience Centre. They were rectified to the same geographic grid as the AVHRR data, but since our interest was with the water colour patterns only, no atmospheric corrections were applied. Band 5 was used to mask cloud and land areas. The images in Plate 5 have been contrast stretched to emphasize the colour variations.

RESULTS AND DISCUSSION

DESCRIPTION OF 1983 WATER COLOUR AND TEMPERATURE PATTERNS

August, 1983

Our fisrt airborne water colour survey was conducted 19-24 August following a period of predominantly easterly winds, and beginning two days after a switch to southerly and southwesterly winds. A NOAA-7 AVHRR thermal image for 14 August 1983 (Plate 1, top) illustrates conditions prevailing before the systematic whale surveys began. Preceding easterly winds had directed the warm Mackenzie River plume to the north and west. Warm water extended along the Yukon Coast and past Kay Point to Herschel Island, isolating a pool of slightly cooler water in the Stokes Point area. (A map showing place names, bottom topography and calibration stations is provided in Figure 32.) The western edge of the warm plume was convoluted and without a strong thermal gradient. An abrupt thermal discontinuity was present northwest of Herschel Island however, presumably caused by upwelling in the lee of the island. Note that the turbid water in Kugmallit Bay had been forced onto the western shore of the bay by the easterly wind. The eastern boundary of this plume was very sharp.

By the time of our airborne operations, the Mackenzie River plume had a much more contracted distribution in eastern Mackenzie Bay probably as a result of the southerly winds on 20 and 21 August (Figures 14-16). It was separated from cooler, less turbid waters offshore by a sharp discontinuity and extended north and east around the edge of the delta as a zone of very bright, grey-brown water visble by eye and in both the satellite and airborne data. Surface temperatures in the turbid water ranged from 12-14°C while the clearer waters just outside the plume were near 9°. Both the airborne water colour data and the 22 August 1983 band 1 image (Plates 2 and 3) show that suspended particulate loads in the plume were greater than 20 $mg \cdot L^{-1}$ (the upper limit of our calibrations based on surface samples). None of the sensors

used here have sufficient gain to sense the lower radiances offshore, but the satellite images in Plates 2, 3 and 4 all emphasize the abruptness of the western edge of the plume after 22 August, and confirm the position of the discontinuity shown in the airborne data.

While our remote sensing methods cannot retrieve chlorophyll a concentrations from these turbid waters, our calibration samples indicate that the chlorophyll a (+ phaeopigment) concentrations in the turbid waters near the Delta and in Kugmallit Bay were in the range 0.5-1.0 $mg \cdot m^{-3}$. From 45-75% of this was live chlorophyll a (see Appendix 4) with the highest percentage being observed near the outer edge of the plume. No bowhead whales were seen in these very turbid waters.

The NOAA and airborne data both show a separate turbid plume issuing from the eastern channel through Kugmallit Bay. By 22 August the turbid plume was situated further east in the bay as a result of southerly winds. A narrow band of bright brown water with SPM in the range 5-10 $mg \cdot L^{-1}$ was also present all along the Tuktoyaktuk Peninsula, separated from darker, less turbid brown-green or green waters further offshore by a sharp discontinuity in some areas and by a more gradual transition in others (Figures 14 and 16). A band of green and green-blue coloured water (G/B 1.0-0.8) extended a further 5-10 km offshore, gradually changing to clear blue waters along the 25 m isobath. Five bowhead whales were observed in blue-green water in this area.

This offshore gradation of water colour was probably mostly a result of suspended sediments, and not chlorophyll. It is not possible to compare water colour and temperature patterns in this area directly, since the AVHRR thermal data in Plates 2 and 3 are from 22 August, one to two days before the eastern transects were flown. Strong and varying winds during this period will have caused substantial water movements.

A sharply delineated patch of very cold water (near 2-3°C) just north of Cape Bathurst (Plate 3, middle) indicated local upwelling there resulting from offshore winds previous to 22 August. A band of cool water is also evident along the Tuk Peninsula, but temperatures there were not as extreme, probably because water depths off the Tuk Peninsula are much less than off Cape Bathurst. No water colour data or whale observations are available for the Bathurst Peninsula upwelling.

In the central part of the study area north of the delta, an extensive green coloured water mass was detectable, exhibiting green/blue reflectance (G/B) slightly greater than 1.0 (Figure 14). This colouration extended from the very turbid Mackenzie River plume in the south, past the northern end of the survey lines between transects H through L. Suspended particulate loads inferred for this area from red reflectance (R 640) and green/red reflectance ratios (G/R) were near 1.0 $mg \cdot L^{-1}$, although some inconsistencies existed between data recorded on different days. The southward inflection of the 1 $mg \cdot L^{-1}$ isopleth along lines K and L may be a real manifestation of the cooler waters seen in this area on 22 August thermal image (Plate 3, top). Because this is at the lower limit of our SPM calibration, the 1 $mg \cdot L^{-1}$ isopleth is shown as a dashed line in Figure 16.

The Fluorescence Line Height (FLH) was very low in this green water mass and we interpret the discolouration as evidence of dissolved or particulate material of riverine origin. CTD data from the four CANMAR drill ships indicated the presence of 4-5 m layer of brackish water with salinity in the range of 8-16 ppt. A subsurface chlorophyll maximum could have been responsible for the green colour; however, our field notes remark that the water over submerged portions of ice floes appeared green, suggesting that the colourant was in the top few metres. Two bowheads were observed in this area, near the northern extension of the 1 $mg \cdot L^{-1}$ SPM isopleth and near a small patch of elevated fluorescence. Cloud in this region on the thermal image does not allow us to see whether the temperature discontinuity visible near 70° continues this far north.

East of line M was a large area of clear, blue water with G/B less than 1.0, decreasing to near 0.75 in the northeast. In this region, the water over submerged in ice appeared blue to the eye. Suspended particulate loads were less than 1 $mg \cdot L^{-1}$ and very low Fluorescence (FLH) and G/B are confirmed by calibration samples having surface chlorophyll concentrations less than 1 $mg \cdot m^{-3}$. Surface salinity at the calibration stations in this blue water were greater than 20 ppt. Fifteen bowhead whales were recorded in this area, roughly distributed along the 50 m isobath and widely dispersed in blue and blue-geen water. Unfortunately we do not have coincident temperature measurement. Most bowheads observed on 23 and 24 August appeared to be in the outer portion of the thermal plume as imaged on 22 August (Plate 3, middle). However, strong southerly winds during the interval may have altered the real relationship.

West of line H, the interpretation of water colour patterns is complicated by the fact that much of the data is of poor quality. Because the data were obtained under very heavy overcast, the incident and upwelling signals were extremely low and electrical noise was a problem. Experience in the eastern Arctic has shown that our incident correction does not work well at these low signal strengths, and the calculated reflectances are elevated. The data no longer follow established calibration relationships. The green/blue reflectance ratio for the first five transects flown on 19 August (A to E) were not useable for this reason. The red reflectance (R 640) was noisy but useable for all but A and B.

In spite of very ragged spectra, a strong fluorescence peak was visible from data obtained near Herschel Island (Figure 17). The exact chlorophyll concentration responsible for this peak cannot be inferred directly from the FLH, but other factors such as the centre wavelength of the fluorescence peak and its shape and size relative to the 560 nm peak are consistent with a surface chlorophyll concentration in the range 2-5 $mg \cdot m^{-3}$.

The G/B, FLH and R 640 were all elevated across a 40-50 km wide band along the Yukon coast, implying increased chlorophyll concentrations and suspended particulate loads in this region. The highest G/B and FLH were in a band 5-10 km offshore, while highest red reflectance was measured over turbid waters close to the coast (Figures 14, 15 and 16). The 22 August thermal data (Plates 2 and 3) clearly show that the water near the coast was very cold (2-3°C compared to near 13°C in the plume and 8-9°C further offshore).

Two relatively cloud-free LANDSAT 4 images were obtained for the western portion of the study zone, to supplement the airborne data and the AVHRR imagery. LANDSAT imagery was not obtained for the other areas. Plate 4 and Figure 18A (bound with Plate 4) are the band 2 (600-700 nm) image for the Yukon coast west of Herschel Island on 20 August 1983 and a line drawing interpretation, respectively. Features of note are a tongue of open pack ice near the coast in the west, small zones of turbid water near the rivers to the west of Herschel Island and a complicated pattern of turbidity fronts in the vicinity of Herschel Island. The Z shaped form attached to Herschel may have been the result of tidal motions or inertial oscillations (caused by the shift of the wind two days earlier) superimposed on other longer term flow. The ice tongue at the left of the image was the leading edge of pack ice moving southeastward into the Canadian Beaufort during late August and early September.

Only three bowhead whales were observed in this area, on a flight made 19 August. One animal was seen at the boundary separating the high chlorophyll zone west of Herschel (Figure 15) from turbid waters closer to shore, while two whales were found in clear waters north of Herschel, within 5 km of a sharp thermal discontinuity crossing the western sector (Plates 2 and 3). In spite of the poor airborne data obtained 19 August on transects A through E, it was possible to map the extent of the turbid water in the vicinity of Herschel Island using the red reflectance and green/red ratio (Figure 16). A zone of high FLH was situated just north of this turbidity and extended around the north side of Herschel, where it was separated from the Island by a sharp front and narrow band of turbid water (also visible in Plate 4)

Plate 4 (bottom) is a LANDSAT 4 band 2 image acquired 22 August 1983 on an orbit further east than that of 20 August. As shown in Figure 18B, more structure is visible in this area because of higher upwelling radiances caused by suspended sediment. The very bright Mackenzie River plume is visible in the east, with a easterly flow clearly indicated by the wakes behind Pelly and Hooper Islands near the delta. The sediment patterns in the vicinity of Herschel and Kay Point are more complicated than two days earlier with a northerly or northeasterly flow indicated. A small ice flow seen near the northern edge of both images also showed a net north-northeastward movement of 25 km during the 48 h interval between images, for an average velocity of approximately 14 $cm \cdot s^{-1}$ or 0.3 knots. Turbidity patterns near Herschel Island are well delineated in the band 2 print and pseudocolour transparencies; however, a linear feature running northwest--southeast is also faintly visible 20-40 km north of the island. Comparing the patterns in the airborne, MSS and AVHRR thermal data we see good agreement in the areal extent and configuation of the temperature and turbidity patterns both near Herschel and further north. Note that unlike the very turbid, high reflectance Mackenzie River plume visible near the delta, the turbid waters near Herschel were cold (near 2.3°C). This fact plus the observed direction of drift, leads us to believe that upwelling from below the shallow (5 m) thermocline was occuring along the Yukon coast on 22 August. The high fluorescence band along the northern side of this cold turbid water and the report by McLaren and Davis (1984) of the presence in the cold water zone of glaucous gulls (Larus hyperboreus) and black-legged kittiwakes (Rissa tridactyla) which are both surface plankton feeders, are consistent with this interpretation. We have no in situ data in this region.

Unfortunately, the location of the large congregation of bowhead whales (85 animals or more) observed near King Point (McLaren and Davis 1984) was cloud-covered at the time of the LANDSAT image. However, the airborne data obtained on two transects that parallel the Yukon coast on 22 August showed that the area between Herschel and Shingle Point was turbid, with suspended particulate loads near 2-3 $mg \cdot L^{-1}$ and Secchi transparency of 1.5-3 m across most of the transects (Figures 19-23). Water colour was variable along the coastal transects, however. Just off King Point a small (5-10 km long) patch of sightly less turbid water was detected coinciding closely with the observation of 80-100 bowhead whales (Figure 20, redrafted from McLaren and Davis 1984 and Figures 21-23). The thermal image for this day shows that this patch was the coldest area of the upwelling water (Plate 3, middle). Visual observations suggested that the turbid water was overlaying much clearer water as a thin layer. McLaren and Davis (1984) noted "circular holes of clear water in the turbid layer where bowheads had dived or surfaced through the turbid waters" which are consistent with a 2-3 m surface layer. It is doubtful however, whether the decreased turbidity inferred from lower G/B and R 640 illustrated in Figures 21 and 22 results from these holes.

September, 1983

By the time of the September airborne surveys, which were carried out between the 6th and the 9th, a large tongue of open pack ice covered most of the Mackenzie Bay and extended eastward along the delta front (Figures 24 and 25). The areal extent of the turbid plume in Mackenzie Bay was much reduced. Our September water colour obsevations indicated that a tongue of clear, blue water ($G/B<0.9$, $SPM<1\ mg \cdot L^{-1}$, chlorophyll$<0.5\ mg \cdot m^{-3}$) accompanied the pack ice, extending almost completely across the study area. When this tongue joined with the clear blue water mass in the northeast sector, a blue water corridor would be formed and a long band of green ($G/B>1.0$) presumably somewhat fresher surface waters would be isolated north of the delta near 70°40'N. A train of internal waves,

feeding along the edge of the Mackenzie River turbidity plume, in a region where temperature and turbidity changed sharply (i.e., a density front with small eddies clearly visible in the band 3 CZCS image, Plate 5, bottom). Plate 5 is a particularly good example of a typical shelf-sea front as described by Simpson (1981). Associated with the boundary between, in this case, the low surface density highly stratified river plume and the higher surface density, more homogeneous water offshore, there should be an along-front quasigeostrophic flow (Figure 31). Slight imbalances between the current shear and the density field result in the small eddies along the front. Upwelling just seaward of the front is responsible for a temperature minimum observed and a convergence at the region of maximum gradient. It is easy to see how such a mechanism might result in increased production at primary and secondary levels and eventually attract higher level consumers such as fish, whales and birds.

Although their apparent movement late in August took many whales further offshore and into much clearer, non-turbid water (less than about 1-2 $mg \cdot L^{-1}$ suspended material), the largest groups were still located in or near temperature gradients around the outer edge of two warm tongues originating in Mackenzie and Kugmallit Bays. A similar situation was seen in August, 1982. Even though the area south of 71°N was intensively overflown, bowheads were only observed near the edge of the continental shelf. The thermal imagery for 26 August 1982 (Plate 8) shows that this coincided with the outer edge of waters warmed by the Mackenzie at that time. From the small number of images examined here, we have no idea how often there is a thermal gradient in the region of the continental shelf.

Upwelling on a local scale may also be an important mechanism in determining the patterns of primary and secondary production in the Beaufort (and hence the distribution of marine fish, birds and mammals). Temperature patterns in several AVHRR images presented earlier give evidence of turbulent circulation near Herschel Island and Cape Bathurst, such as has been described by Takahashi et al. (1981) in the lee of an island in a coastal current. While some whale surveys have been done near Cape Bathurst, we did not obtain any imagery coincident with surveys. Whales do seem to congregate there on occasion, however. For instance, systematic surveys during September, 1981, show that small groups of bowheads were aligned all along the coast of the peninsula about 15 km offshore (Davis et al. 1982). Strong thermal and turbidity fronts in the same area and in nearly the same orientation are seen in the 26 August and 13 September 1982 and 22 August 1983 imagery. Fraker and Bockstoce (1980) also concluded that the Cape Bathurst area is important for bowheads in late summer. We suggest the physical circulation in the area may be the ultimate causative factor.

Any flow along the Yukon-Alaska coast will tend to cause turbulent motions in the lee of Herschel Island. The 14 August 1983 thermal image (Plate 2) shows an example after several days of strong easterly winds. By the time of the 1983 airborne surveys, the winds were more southerly and therefore upwelling was possibly responsible for the cold water along the Yukon coast also. Bowhead whales are often found in the region of Herschel Island (Richardson 1983) and while there are relatively few data, it is reasonable to expect elevated phytoplankton production in such areas of intermittent mixing and stabilization. The oceanography of this region should be examined in more detail since it appears to be of some biological importance.

Our airborne surveys were conducted late in the Arctic summer and it is therefore understandable that we detected little surface chlorophyll anywhere but near possible local sources of nutrients, since most of the southern Beaufort is strongly stratified (Herlinveaux and de Lange Boom 1976). On the August surveys the only chlorophyll we detected was in the cold water west of Herschel (the imagery is not coincident with our flight) and along the offshore (downstream) edge of the upwelled water off King Point. A band of slightly elevated fluorescence just north of the very turbid water near Richards Island may also be significant. If the Mackenzie River is supplying nitrogen (Grainger 1975) then the plume edge should be a region of increased phytoplankton growth under some circumstances. Cells limited in the stratified, very turbid river water by light might be expected to grow in a transition zone near the edge of the plume where the turbidity decreases due to settling out of suspended particles. Grainger's (1975) zooplankton data showed a mixture of marine and freshwater zooplankton in this part of the plume. The fact that the CZCS image (Plate 5, bottom) shows a stepped rather than gradual decline in brightness, may mean that certain euryhaline phytoplankton species might find elevated nutrient concentrations there with at least temporary stratification and enough light to grow. Recent data from the region of Issungnak (Erickson et al. 1983) indicate that the river is not a strong source of nitrate, however. This probably means that phytoplankton growth along the plume will only be significant in late summer when the nutrient concentrations offshore have been reduced to near zero. More comprehensive *in situ* studies are needed, however, before this is anything more than speculation.

It is interesting that the 1980-83 distribution studies appear to show a progressive offshore shift in bowhead abundance (Richardson 1983). There clearly has been a change from feeding along the edge of the turbidity plume in shallow waters (1980) to feeding near thermal discontinuities further offshore (1982) or to potentially zooplankton-rich areas away from the main industrial zone (1983 upwelling near the Yukon coast). Although there is a permanent turbidity/temperature front over the shallow waters just north of Richards Island and Kugmallit Bay, bowhead whales have not always been observed there consistently. Their abundance in 1976, 1977, 1978 and 1980 and absence in 1979, 1981, 1982 and 1983 could be related to zooplankton abundance. Our data do not resolve the existing questions concerning bowhead distribution, but they provide indirect support for the suggestion that zooplankton abundance is probably a determining factor.

CONCLUSIONS

The 1983 airborne water colour data showed that significant amounts of chlorophyll a can be produced in the Beaufort as late as the end of August, where local wind-induced upwelling occurs. The small number of satellite thermal images examined from 1980-1982 suggests that such upwelling commonly occurs near Herschel Island and Cape Bathurst in August and September. Bowhead whale distribution in August, 1983, further suggests that such local upwelling can be important areas of whale concentrations under some circumstances. The recurring polynya off Cape Bathurst indicates upwelling there during the winter. Since we have not examined imagery from other times of the year we therefore have no information on upwelling earlier in the summer. However, if small local upwellings are frequent throughout the season the Beaufort may be more productive than was previously thought.

Congregations of bowheads were also found to be associated with temperature and/or turbidity discontinuities seen in satellite images from all four years. Previous studies elsewhere have demonstrated that such fronts are often the site of production, with large numbers of zooplankton accumulated near them.

Future work on the ecology of the Beaufort should include an examination of the primary and secondary production of the fronts and gradients associated with the Mackenzie River plume.

The airborne instrumentation and techniques as used in 1983 are capable of producing useful data even under severe conditions. Modifications to the instrumentation currently underway will greatly improve its performance. Digital satellite data can provide very valuable information describing the temporal and spatial variability of temperature, turbidity and water colour over the whole region. All three parameters appear to be important direct or indirect determinants of animal distribution in this area.

SUMMARY

1. Data collected, summer/fall 1983
   Water colour variation over a 4000 square km area of the southern Beaufort Sea were mapped coincident with the 1983 bowhead whale survey conducted for the Environmental Studies Revolving Fund (DIAND) by LGL Ltd. during 19-24 August and 6-9 September 1983. Airborne measurements of spectral reflectance and in vivo fluorescence of chlorophyll a were conducted using the I.O.S. colour spectrometer. Coincident satellite data drescribing thermal and sediment pattersn were also analysed.
2. Comparison of thermal and turbidity fields with bowhead distribution 1980-1982
   Several examples of satellite imagery acquired over the southern Beaufort during August and September, 1980-1982, were also analysed and the thermal and turbidity fields were compared to the distribution of bowhead whales observed over short periods corresponding to the time of each image.
3. Water colour and temperature variations in the Beaufort Sea
   Strong water colour and temperature variations exist in the southern Beaufort Sea and distinctive signatures permit separation, identification and tracking of Mackenzie River water, clear more saline offshore water, recently upwelled water and zones of concentrated phytoplankton using remote sensing techniques.
4. Bowhead whales, water colour and temperature: August, 1983
   During 19-24 August 1983 the warm (>13°C), low salinity (<10 ppt), very turbid river water (>10 $mg \cdot L^{-1}$) was held close to the delta by westerly and southerly winds. Surface chlorophyll concentrations were less than 1 $mg \cdot m^{-3}$ everywhere in the study zone except off the Yukon coast, where evidence suggests a local upwelling was in progress. Surface temperatures near the coast were near 2°C and a band of greatly elevated chlorophyll fluorescence was located along the offshore edge of this cold water mass. Large numbers of bowheads were concentrated in this upwelled water. A more diffuse group was observed 60-100 km off the Tuktoyaktuk Peninsula near the outer edge of the thermal plume originating from the Mackenzie River.
5. Bowheads, water colour, temperature: September, 1983
   Pack ice covered much of the southern Beaufort during 6-9 September 1983. The extent of the zone apparently influenced by the river was decreased. Suspended sediment concentrations near the coast were much lower than in August and surface chlorophyll concentrations were low everywhere. The largest group of bowhead whales observed was widely dispersed throughout cold clear waters in the northeast part of the study zone.
6. Bowheads, water colour, temperature: 1980-1982
   Five satellite images for August and September 1980-1982 demonstrated that important congregations of bowhead whales (and many smaller groupings also) tend to occur in the vicinity of oceanographic discontinuities manifesting themselves as surface temperature or turbidity fronts. Other studies have shown that zooplankton abundance in such areas is usually higher than in more homogeneous areas nearby.

RECOMMENDATIONS

1. Extend whale/imagery comparison
   A large amount of historical satellite data exists. These archives should be thoroughly searched for cloud-free imagery of the southern Beaufort Sea and North Alaskan slope for all of the open-water season and the useful digital data obtained. Satellite imagery should then be merged with as much historical in situ physical, chemical and biological data as

(ed.) Manual of remote sensing. 2nd ed. Vol. 2. Interpretation and applications. American Society of Photogrammetry, Falls Church, VA. 2240 p.

LJUNGBLAD, D.K., S.E. MOORE, D.R. Van SCHOIK, and C.S. WINCHELL. 1982. Aerial surveys of endangered whales in the Beaufort, Chukchi and northern Bering Seas. Tech. Doc. 486, Naval Ocean Systems Center, San Diego, CA. 406 p.

LORENZEN, C.J. 1967. Vertical distribution for chlorophyll and phaeopigments: Baja California. Deep-Sea Res. 14: 735-745.

MACKAS, D.L., G.C. LOUTTIT, and M.J. AUSTIN. 1980. Spatial distribution of zooplankton in British Columbia coastal waters. Can. J. Fish. Aquat. Sci. 37: 1476-1487.

MacNEILL, M.R., and J.F. GARRETT. 1975. Open water currents. Beaufort Sea Technical Report No. 17. Beaufort Sea Project, Department of the Environment, Victoria, BC.

MARKO, J. 1975. Satellite observations of the Beaufort Sea ice cover. Beaufort Sea Technical Report No. 34. Beaufort Sea Project. Department of the Environment, Victoria, BC.

McLAREN, P.L., and R.A. DAVIS. 1984. Distribution of bowhead whales and other marine mammals in the southeast Beaufort Sea, August - September 1983. Unpublished report by LGL Ltd., Toronto for Dome Petroleum Limited and Gulf Canada Resources Inc., Calgary. 65 p.

MILLER, J.R., K.S. GORDON, and D. KAMYKOWSKI. 1976. Airborne water-colour measurements off the Nova Scotia coast. Can. J. Remote Sens. 2: 42-47.

MOREL, A. 1980. In-water and remote measurements of ocean colour. Boundary-Layer Meteorol. 18: 177-202.

MOREL, A., and L. PRIEUR. 1977. Analysis of variations in ocean colour. Limnol. Oceanogr. 24: 709-722.

NEVILLE, R.A., and J.F.R. GOWER. 1977. Passive remote sensing of phytoplankton via chlorophyll a fluorescence. J. Geophys. Res. 82: 3487-3493.

PELLETIER, B.R. 1975. Sediment dispersal in the southern Beaufort Sea. Beaufort Sea Technical Report 25a. Beaufort Sea Project. Department of the Environment, Victoria, BC. 80 p.

PINGREE, R.D., P.R. PUGH, P.M. HOLLIGAN, and G.R. FORSTER. 1975. Summer phytoplankton blooms and red tides along tidal fronts in the approaches to the English Channel. Nature (Lond.) 258: 672-677.

RICHARDSON, W.J. (ed.) 1983. Behavior, disturbance and distribution of bowhead whales Balaena mysticetus in the eastern Beaufort Sea, 1982. Unpublished report by LGL ecological research associates Inc., Bryan, TX for U.S. Minerals Management Service, Reston, VA. 357 p.

ROBINSON, I.S., N.C. WELLS, and H. CHARNOCK. 1984. The sea surface thermal boundary layer and its relevance to the measurement of sea surface temperature by airborne and spaceborne radiometers. Int. J. Remote Sens. 5: 19-45.

SIMPSON, J.H. 1981. The shelf sea fronts: implications of their existence and behavior. Philos. Trans. R. Soc. Lond. A. Math. Phys. Sci. 302: 531-546.

STRICKLAND, J.D.H., and T.R. PARSONS. 1972. A practical handbook of sea water analysis. Fish. Res. Board Can. Bull. 167: 130 p.

STURM, B. 1981. Ocean colour remote sensing and quatitative retrieval of surface chlorophyll in coastal waters using Nimbus CZCS data, p. 267-280. In J.F.R. Gower (ed.) Oceanography from space. Plenum, New York.

TABATA, S., and J.F.R. GOWER. 1980. A comparison of ship and satellite measurements of sea surface temperatures off the Pacific coast of Canada. J. Geophys. Res. 85: 6636-6648.

TAKAHASHI, M., Y. YASUOKA, M. WATANABLE, T. MIYASAKI, and S. ICHIMURA. 1981. Local upwelling associated with vortex motion off Oshimura Island, Japan, p. 119-124. In F.A. Richards (ed.) Coastal upwelling. American Geophysical Union, Washington, DC.

WALKER, G.A.H., V.L. BUCHHOLZ, D. CAMP, B. ISHERWOOD, J. GLASPEY, R. COUTTS, A. CONDAL, and J.F.R. GOWER. 1974. A compact multichannel spectrometer for field use. Rev. Sci. Instrum. 45: 1349-1352.

WALKER, G.A.H., V.L. BUCHHOLZ, D. CAMP, B. ISHERWOOD, and J.F.R. GOWER. 1975. A silicon diode array spectrometer for ocean colour monitoring. Can. J. Remote Sens. 1: 26-30.

WALLACE, J.M., and P.V. HOBBS. 1973. Atmospheric sciences, an introductory survey. Academic Press, New York. 467 p.

WOODWARD-CLYDE CONSULTANTS. 1982. Beaufort Sea sediment dynamics. Unpublished report for Geological Survey of Canada, Dartmouth, NS.

YENTSCH, C.S., and D.W. MENZEL. 1963. A method for the determination of phytoplankton chlorophyll and phaeophytin by fluorescence. Deep Sea Res. 10: 221-231.

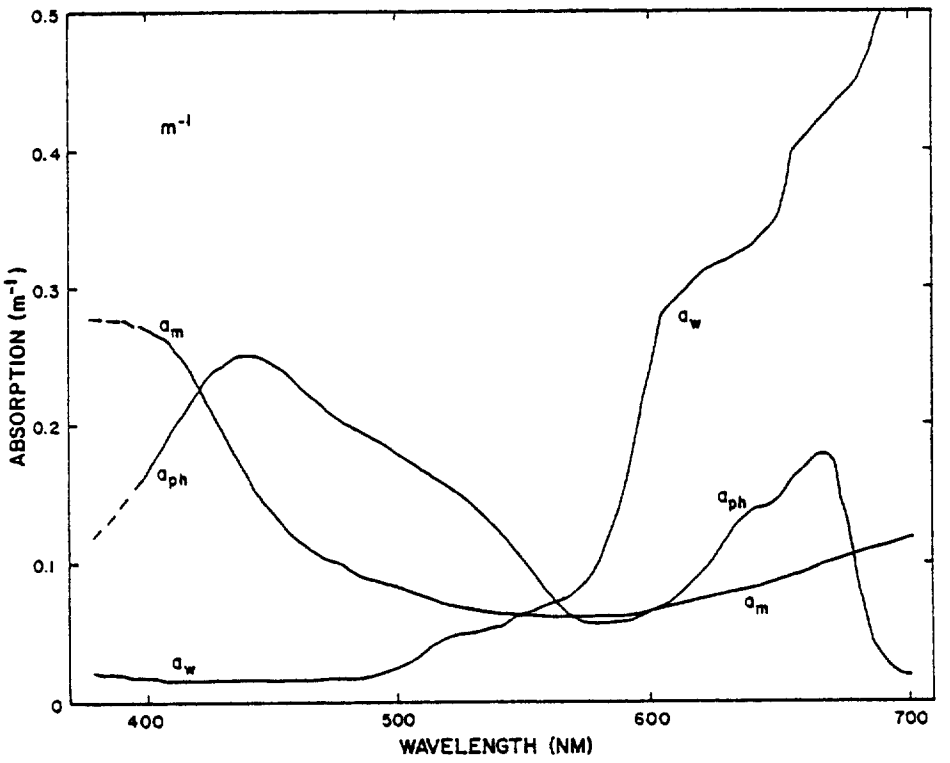

Fig. 1. Spectral absorption by water (a_w), phytoplankton chlorophyll (a_{ph} for 10 $mg \cdot m^{-3}$) and other suspended and dissolved materials. After Morel and Prieur (1977).

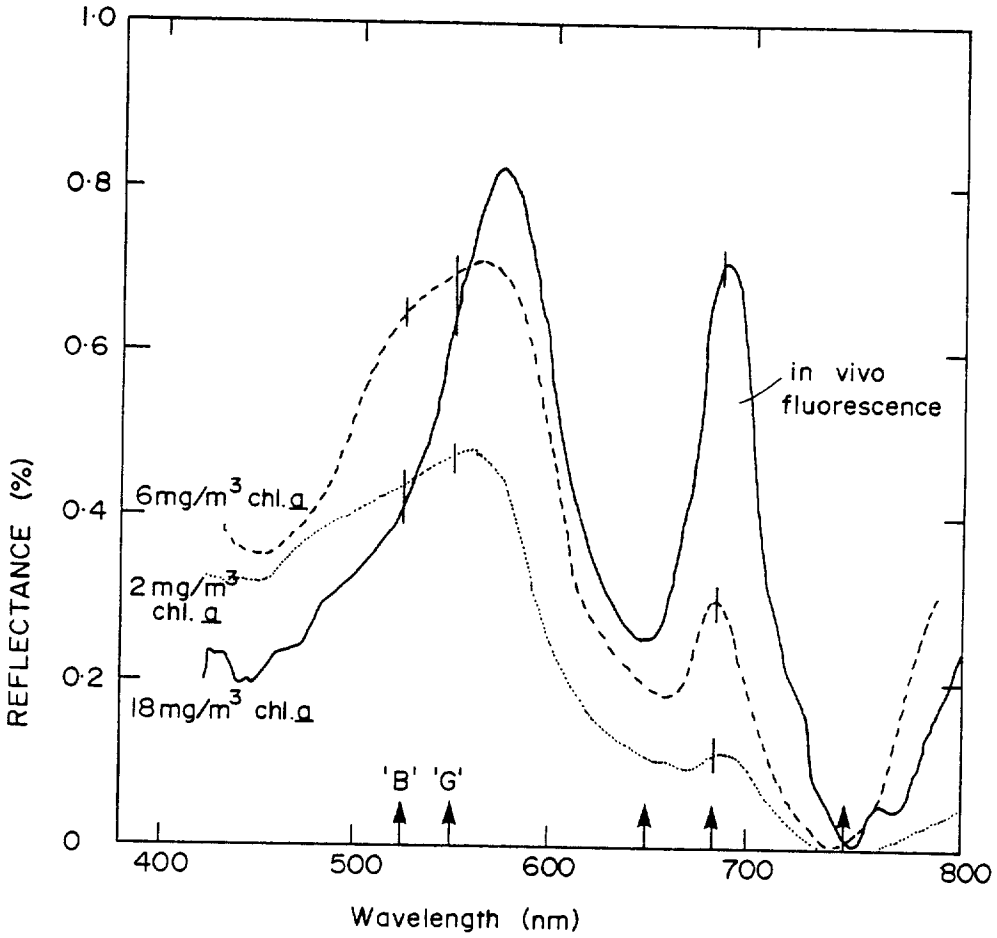

Fig. 2. Reflectance spectra for three locations in coastal British Columbia waters exhibiting different chlorophyll concentrations (values for chlorophyll concentration are averaged for 0-5 m layer). Arrows along the bottom of the figure indicate the wavelengths used in the calculation of the Green/Blue Ratio (G/B) and the Fluorescence Line Height (FLH). From Borstad and Brown (1981).

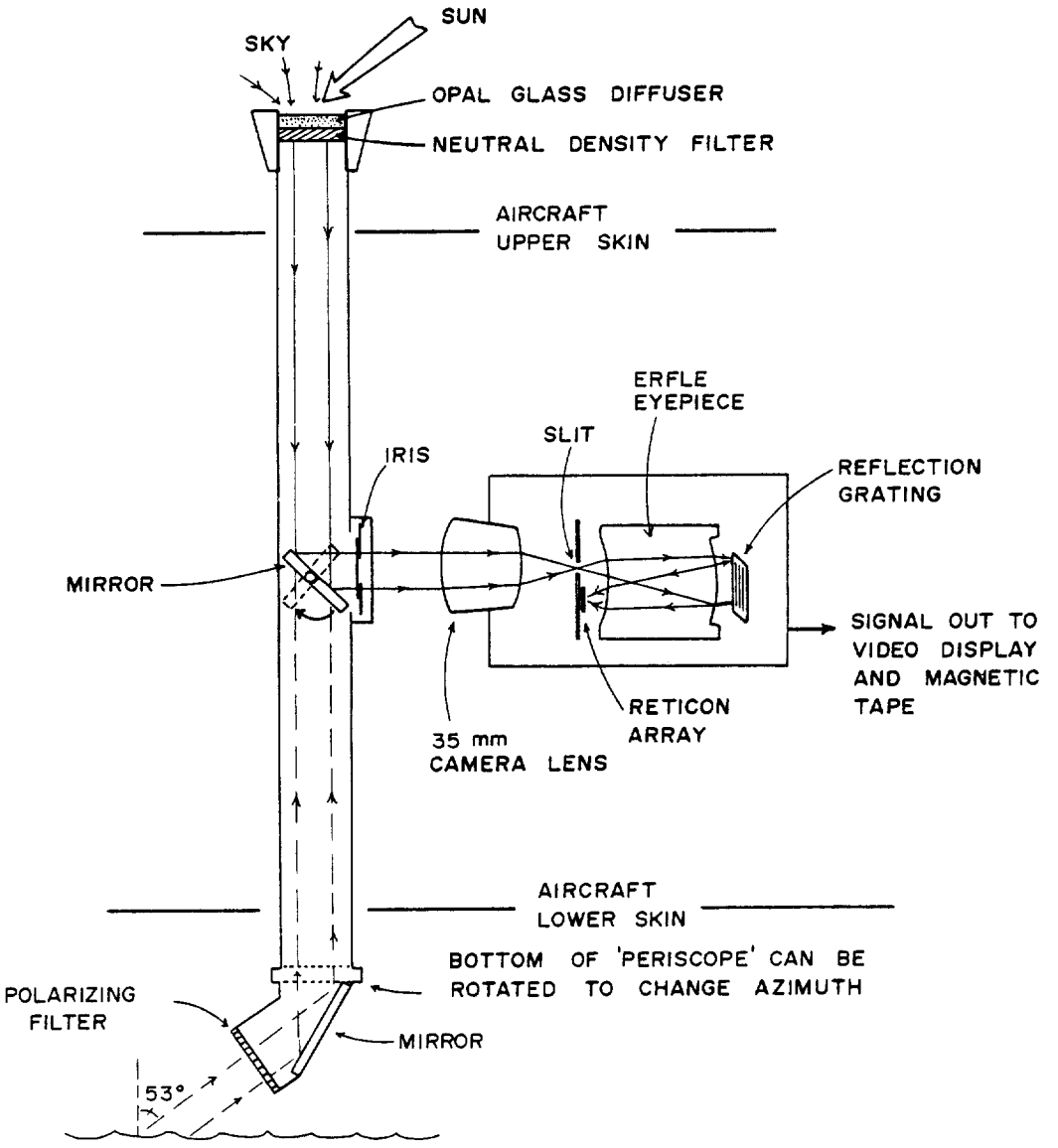

Fig. 3. Schematic representation of the I.O.S. spectrometer as utilized for these surveys (not to scale). The mirror position shown is for measurement of the upwelling spectrum. Incident signals were continuously monitored using a separate, single uplooking photodiode (not shown) and periodically by the spectrometer.

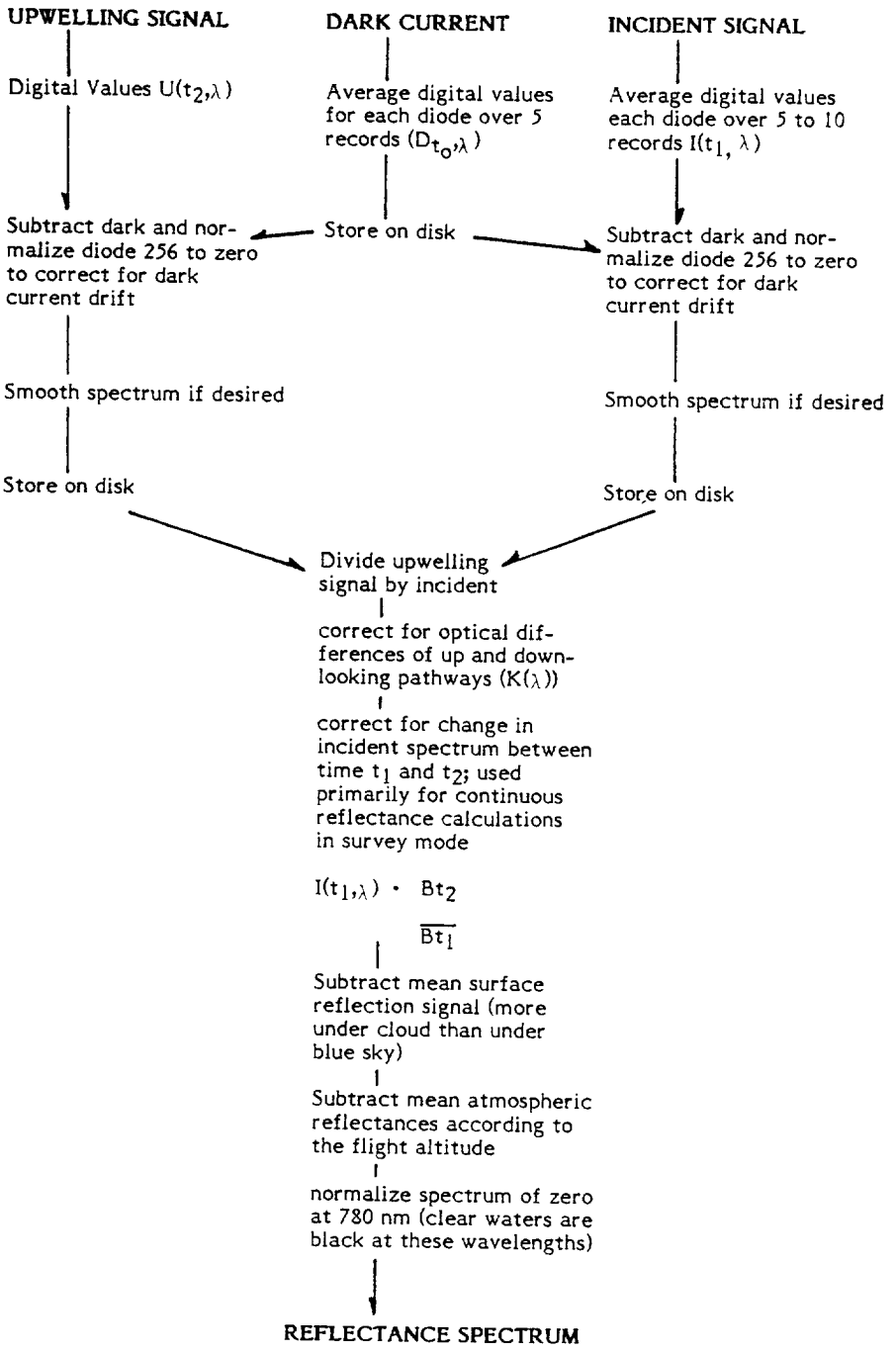

Fig. 4. Summary of data flow and manipulations required for calculating a single reflectance spectrum. For multiparameter stripcharts along the track of the aircraft, spectral upwelling data are not initially averaged. In this case only data from the diodes used in the various indices are handled.

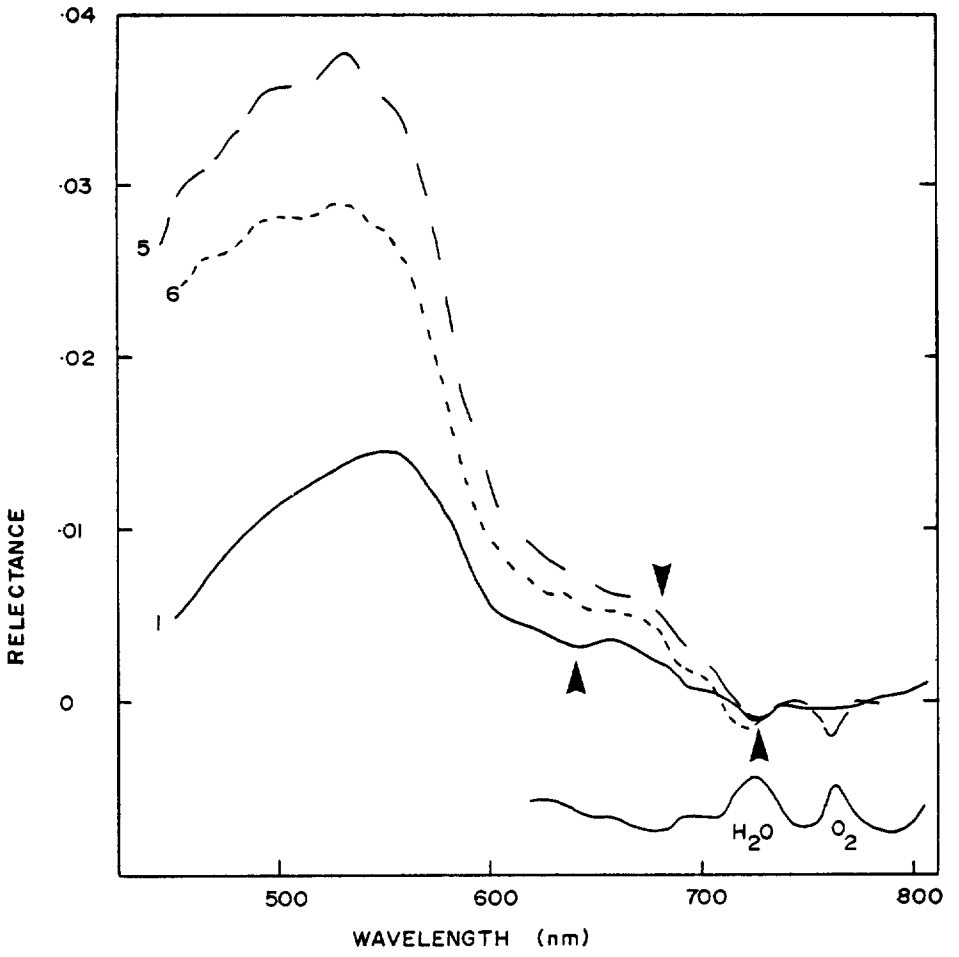

Fig. 5. Examples of reflectance spectra obtained 21 August 1983 in the vicinity of a fog bank. High humidity results in strong absorption lines at 760 nm (oxygen) and 725 nm (water vapour). Current FLH calculations which utilize the wavelengths indicated by arrows are grossly affected.

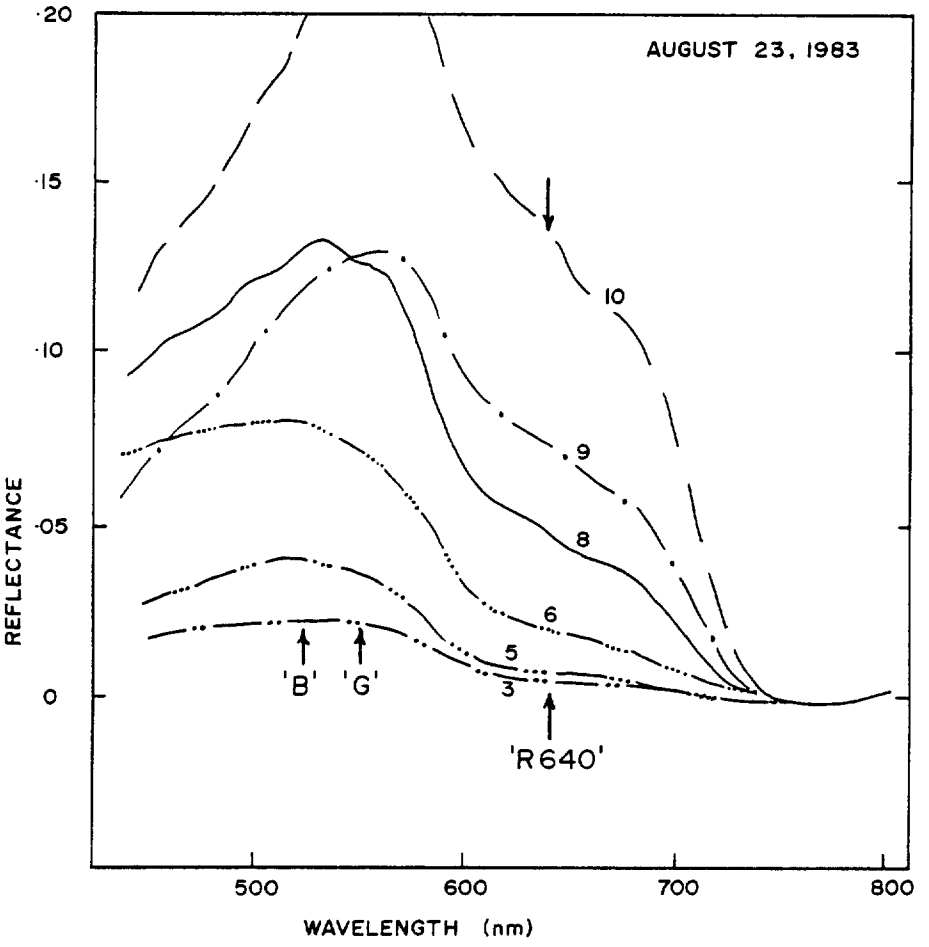

Fig. 6. Examples of reflectance spectra obtained during the 23 August 1983 calibration exercise on a line north of Tuktoyaktuk. B, G and R640 indicate wavelengths of G/B and R640 indices. Numbers on spectra represent stations numbered from north to south (see Figure 32).

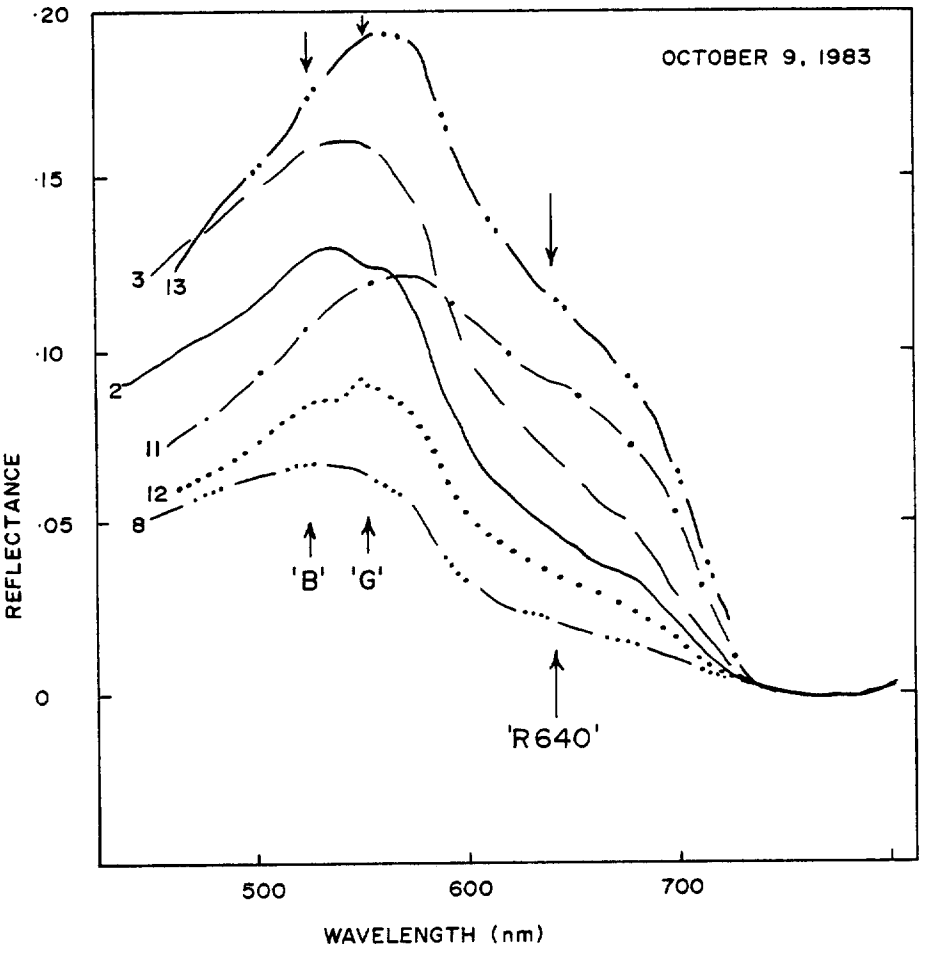

Fig. 7. Examples of reflectance spectra obtained during the 9 October 1983 calibration exercise in the Eskimo Lakes and Liverpool Bay. B, G and R640 indicate wavelengths of G/B and R640 indices. Numbers on spectra represent stations numbered from west to east (see Figure 32).

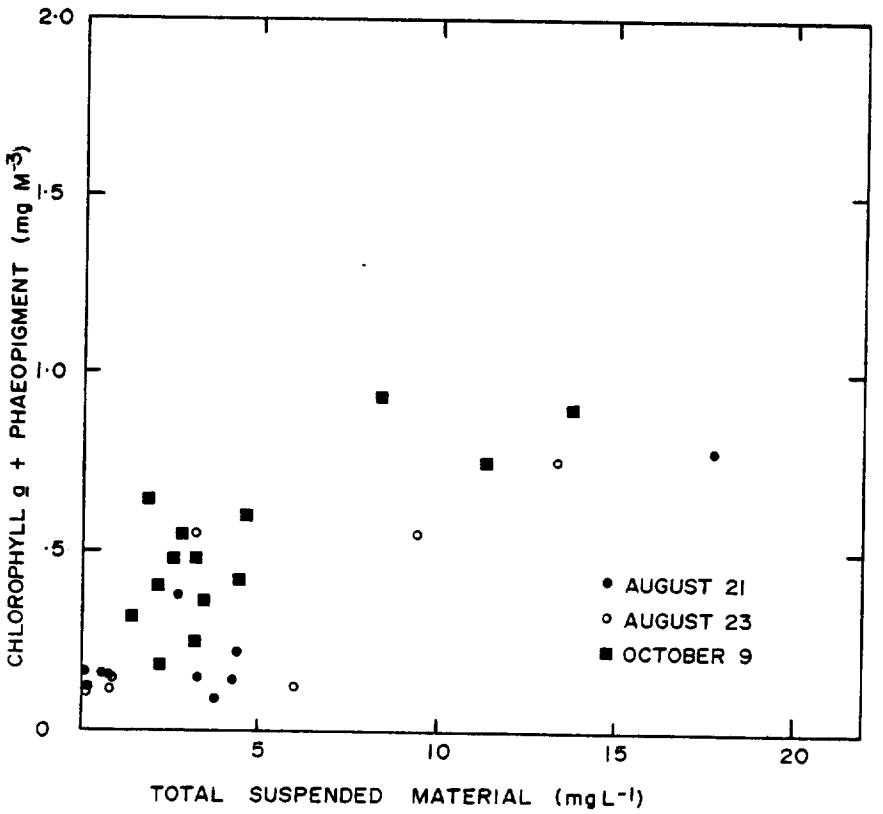

Fig. 8. A comparison of surface chlorophyll a (+ phaeopigment) concentration and total suspended particulate material for all 39 calibration samples.

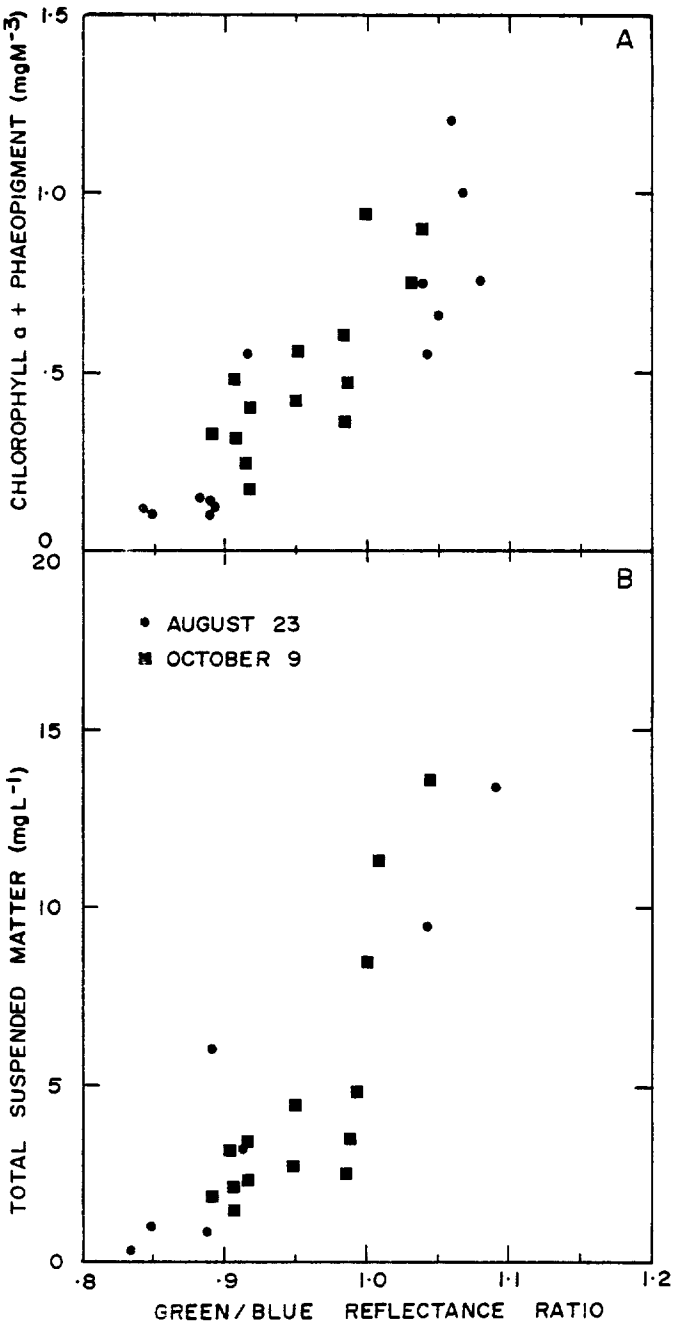

Fig. 9. a) Comparison of surface chlorophyll (C+P) concentration and the calculated green/blue reflectance ratio (G/B) for the 23 August and 9 October calibration exercises.

b) Comparison of the weight of suspended particulate material (SPM) in surface samples and the calculated green/blue reflectance ratio (G/B) for the 23 August and 9 October calibration exercises.

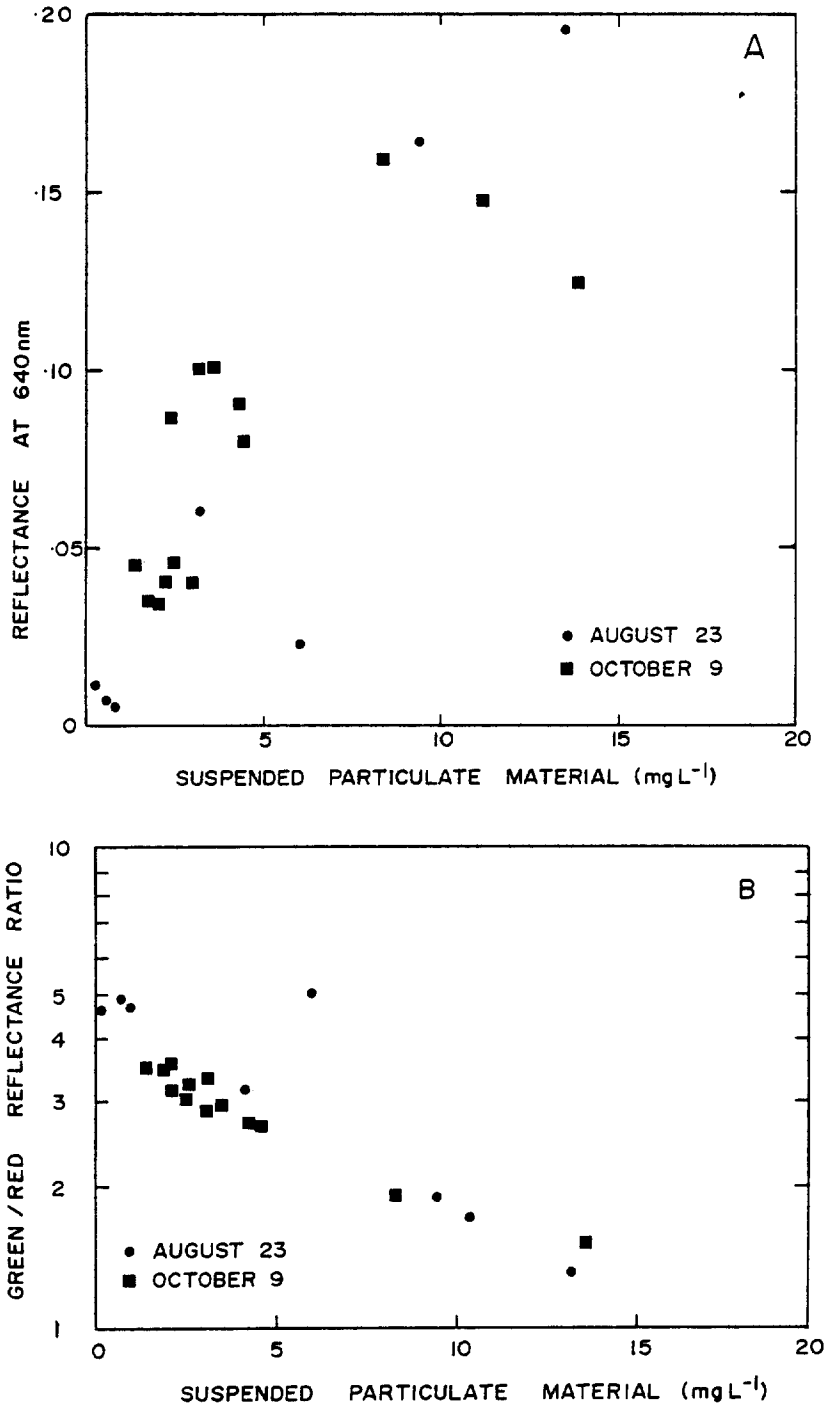

Fig. 10. a) Comparison of the weight of suspended particulate material (SPM) and the reflectance at 640 nm (R640) for the 23 August and 9 October calibration exercises.

b) Comparison of the weight of suspended particulate material (SPM) and the green/red reflectance ratio (G/R) for the 23 August and 9 October calibration exercises.

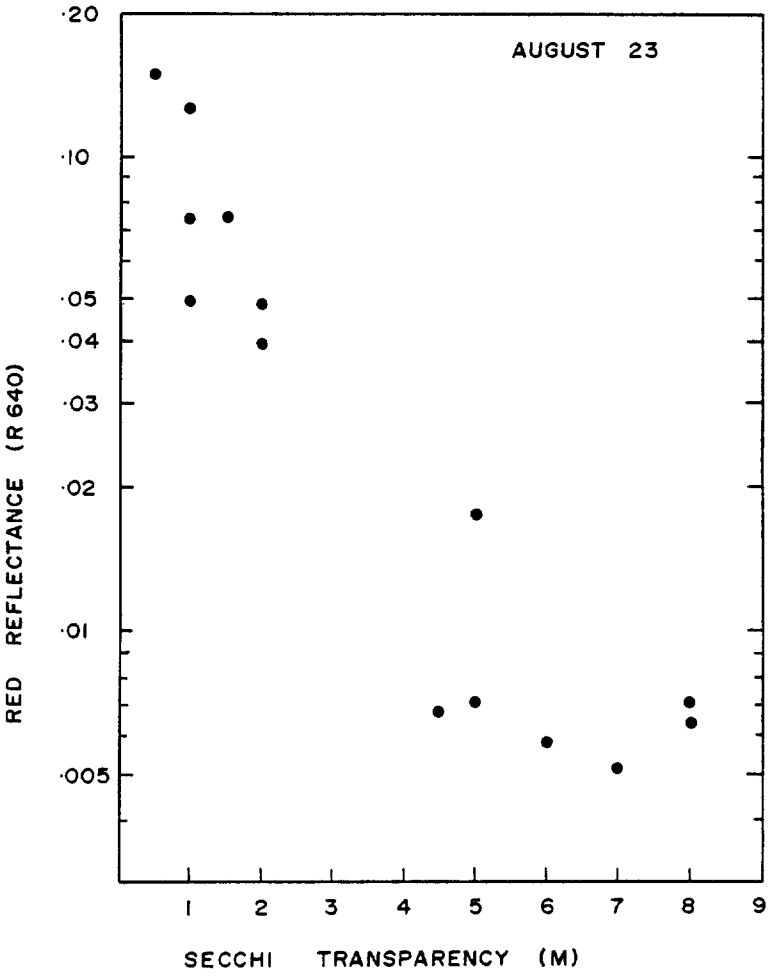

Fig. 11. Comparison of the reflectance at 640 nm (R640) and Secchi depth for the 23 August calibration exercise.

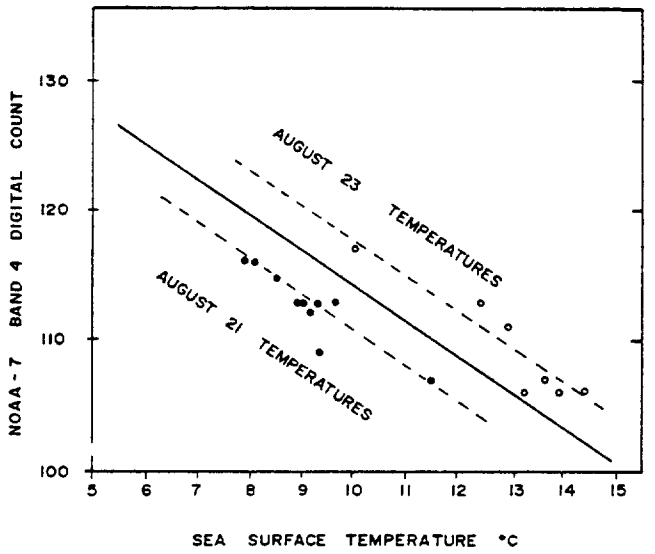

Fig. 12. Comparison of NOAA-7 AVHRR band 6 (thermal infra-red) raw digital counts for 22 August 1983 image with sea surface temperature data obtained 21 and 23 August 1983. Offset between 21 and 23 shows the result of varying atmospheric interference.

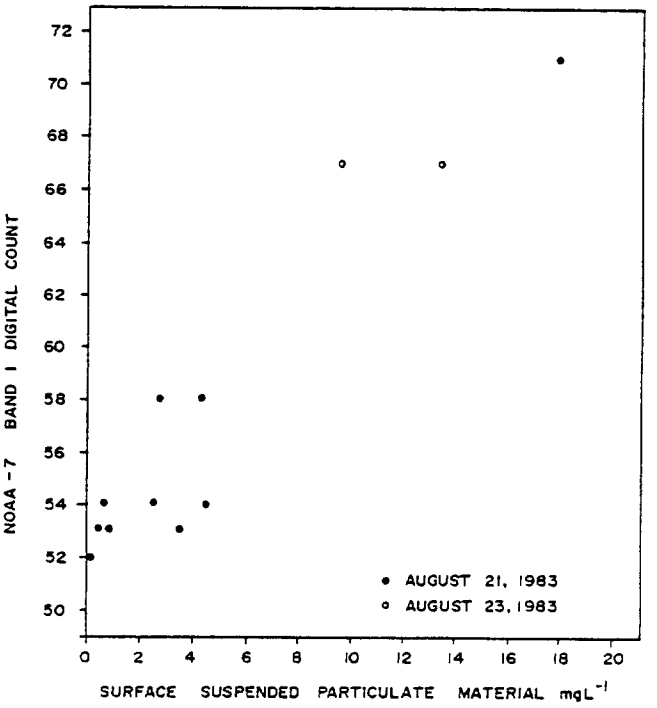

Fig. 13. Comparison of NOAA-7 AVHRR band 1 (visible range) raw digital counts for 22 August 1983 image with weight of suspended particulate matter in surface samples obtained 21 and 23 August 1983.

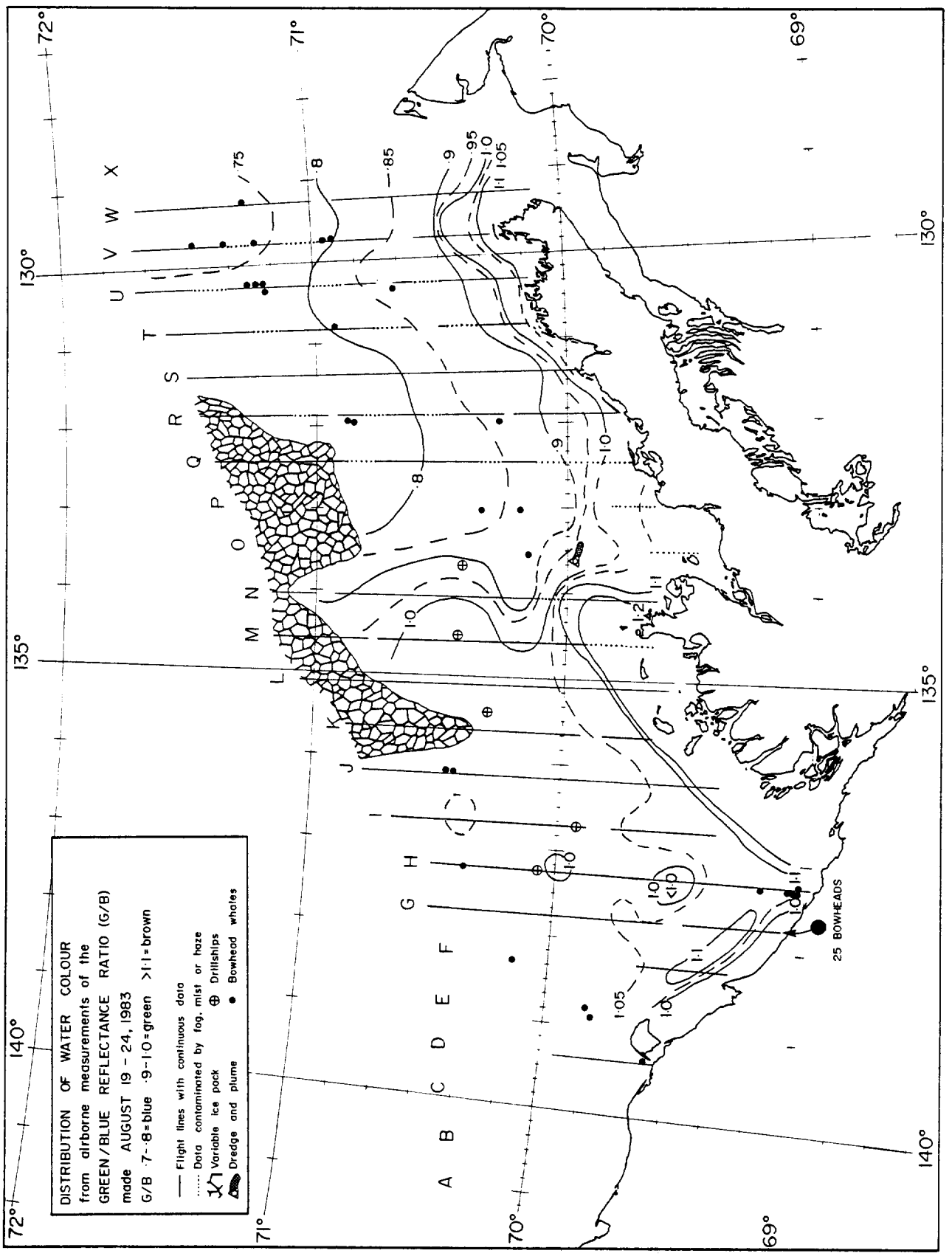

Fig. 14. Distribution of water colour in the southern Beaufort Sea, 19-24 August 1983 as indicated by airborne measurements of the Green/Blue reflectance ratio (G/B).

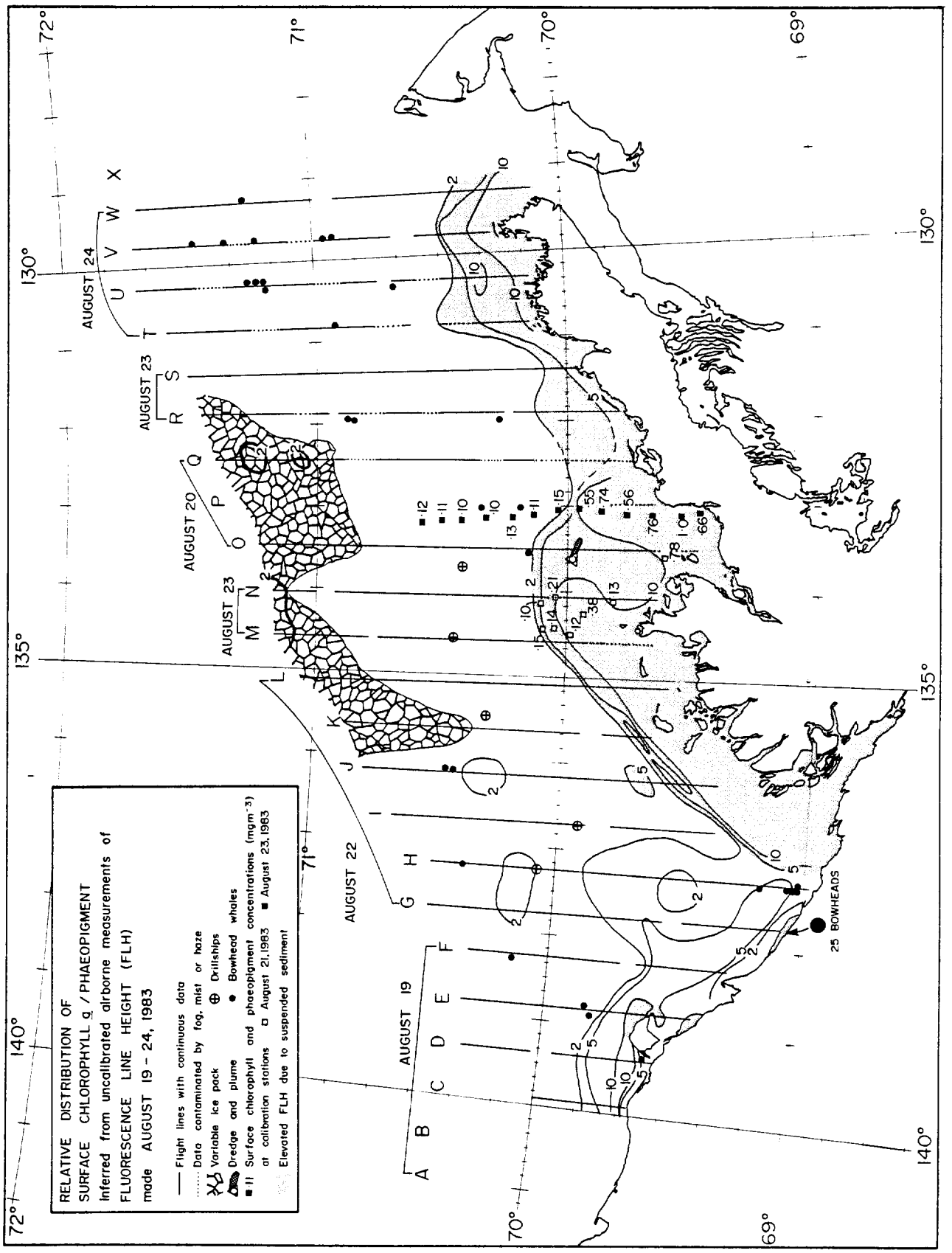

Fig. 15. Relative distribution of surface phytoplankton chlorophyll in the southern Beaufort Sea, 19-24 August 1983 as indicated by uncalibrated airborne measurements of the Fluorescence Line Height (FLH). FLH units are percent reflectance increase × 10.

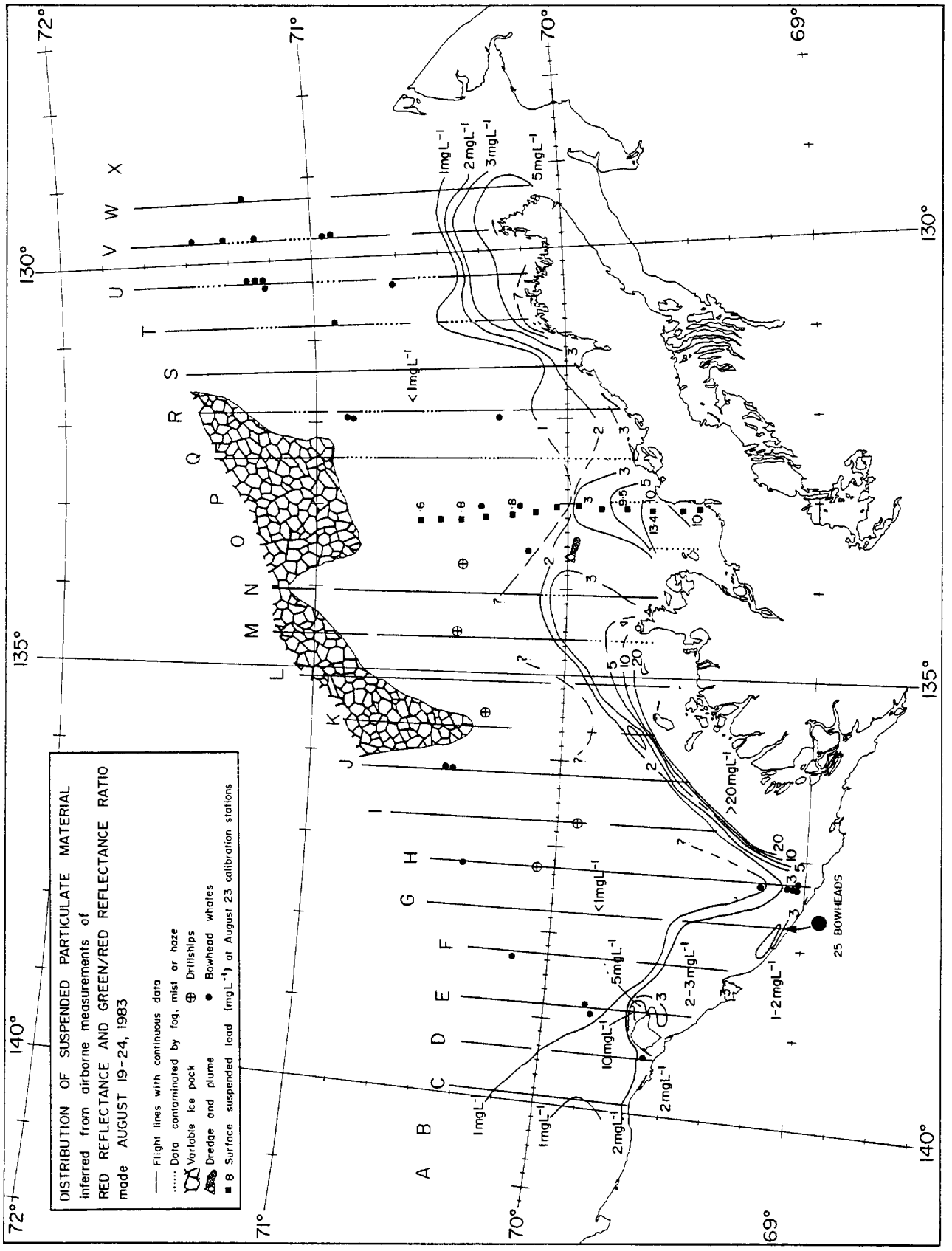

Fig. 16. Distribution of Suspended Particulate Material (SPM) in the southern Beaufort Sea 19-24 August 1983 as airborne measurements of Red Reflectance (R640) and the Green/Red Reflectance Ratio (G/R).

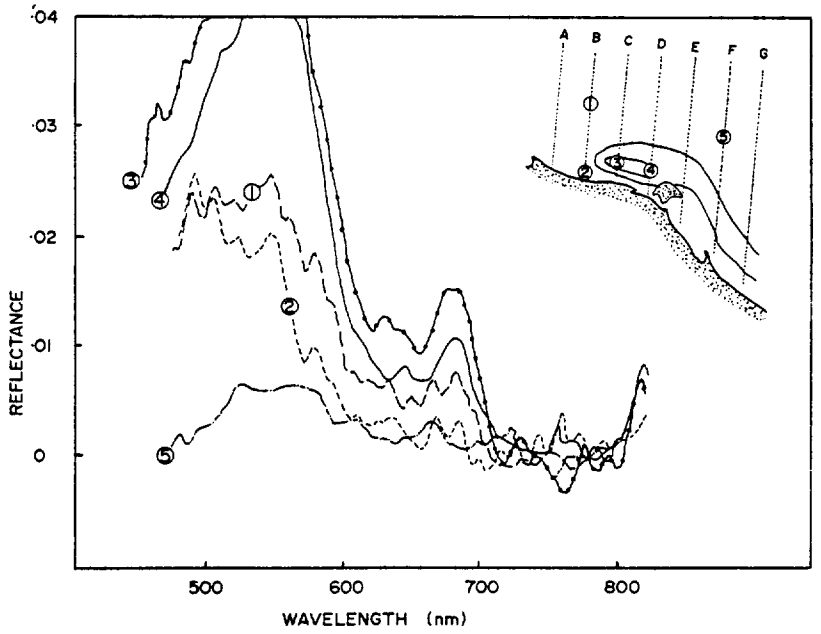

Fig. 17. Representative reflectance spectra obtained 19 August 1983 in the vicinity of Herschel Island. Extremely low light levels resulted in very noisy data, but a large FLH peak is clearly evident near 685 nm.

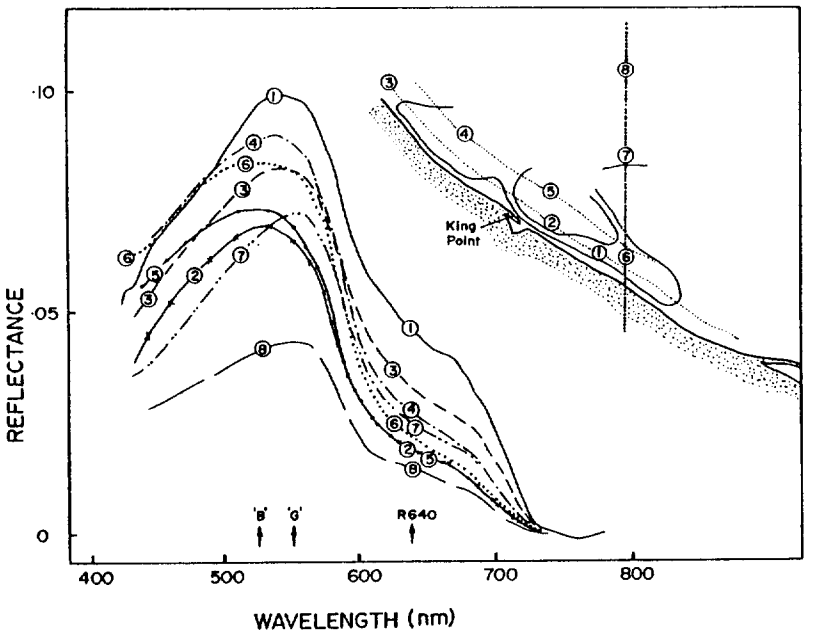

Fig. 19. Representative reflectance spectra illustrating water colour variations in the King Point area 22 August 1983. Isopleths on inset figure are for red reflectance (R640).

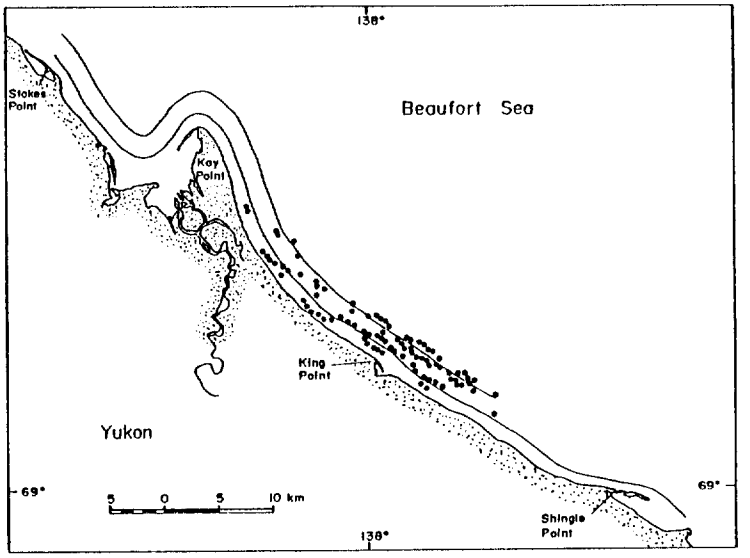

Fig. 20. Distribution of bowhead whales observed by McLaren and Davis (1984) along the Yukon coast in the vicinity of King Point. Dotted lines indicate survey transects; symbols represent locations of individual animals sighted.

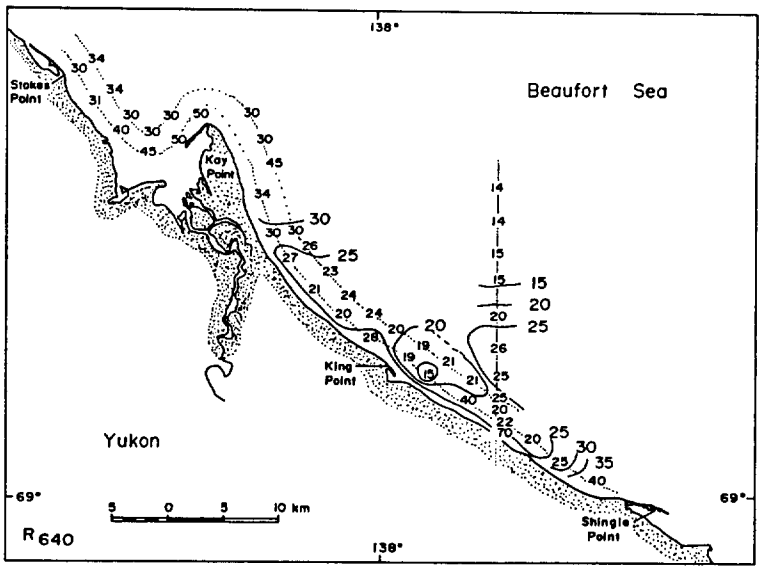

Fig. 21. Variations of red reflectance in the vicinity of King Point 22 August 1983. Values plotted are R640 × 1000 (i.e. 25 = 0.025). Waters having R640 greater than about 0.015 are visibly turbid to the eye.

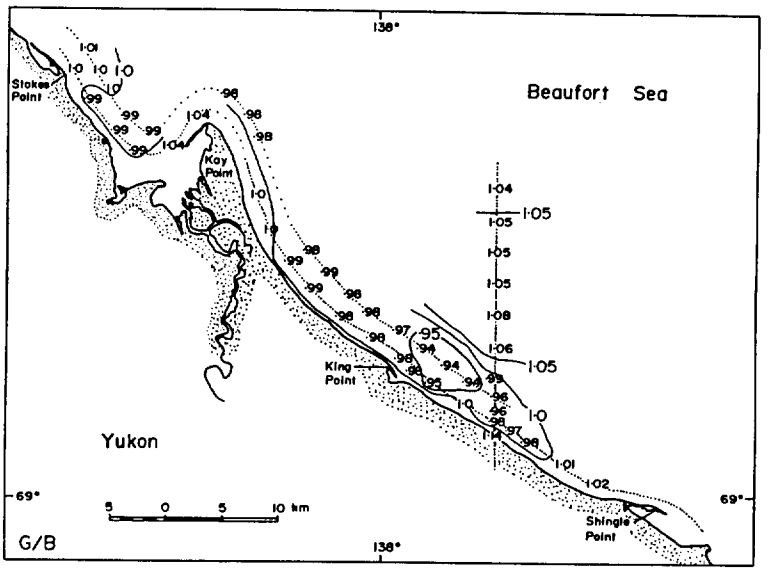

Fig. 22. Variations of water colour as measured by the green/blue reflectance ratio (G/B) in the vicinity of King Point 22 August 1983. G/B index increases from blue to brown. All of this area would have appeared green to the eye.

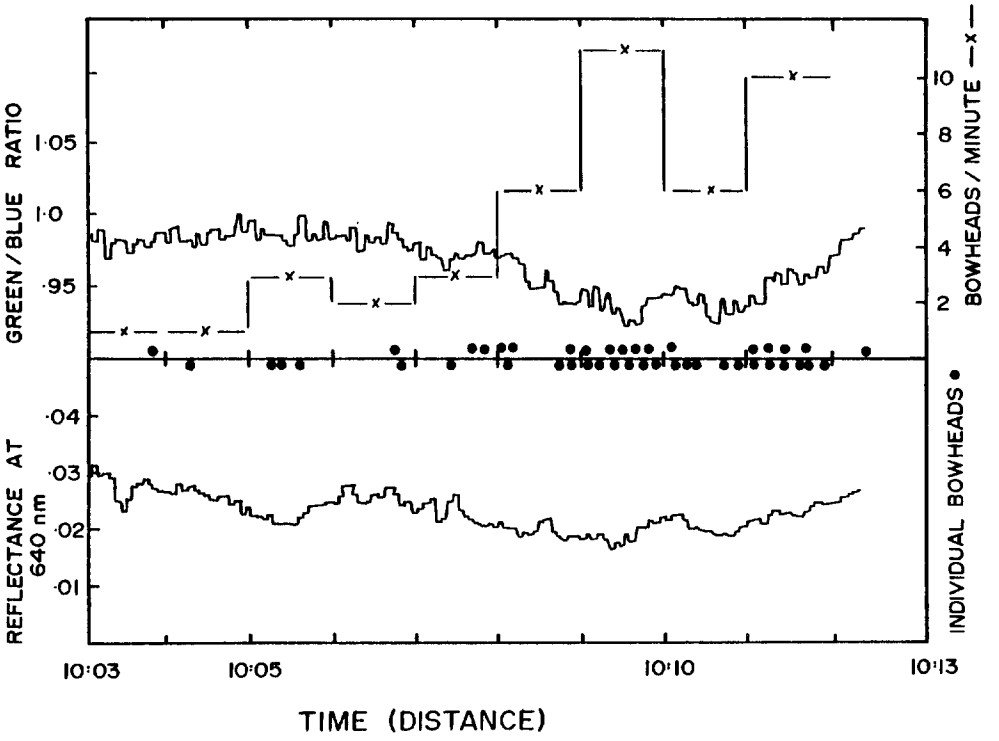

Fig. 23. Comparison of water colour indices with the number of bowhead whales observed by McLaren and Davis (1984) on 22 August 1983 along the eastern portion of the outer transect (closely spaced dotted line in Figures 19, 20). Most whales were seen in water having lowest green/blue ratio and red reflectance, that is the lowest turbidity.

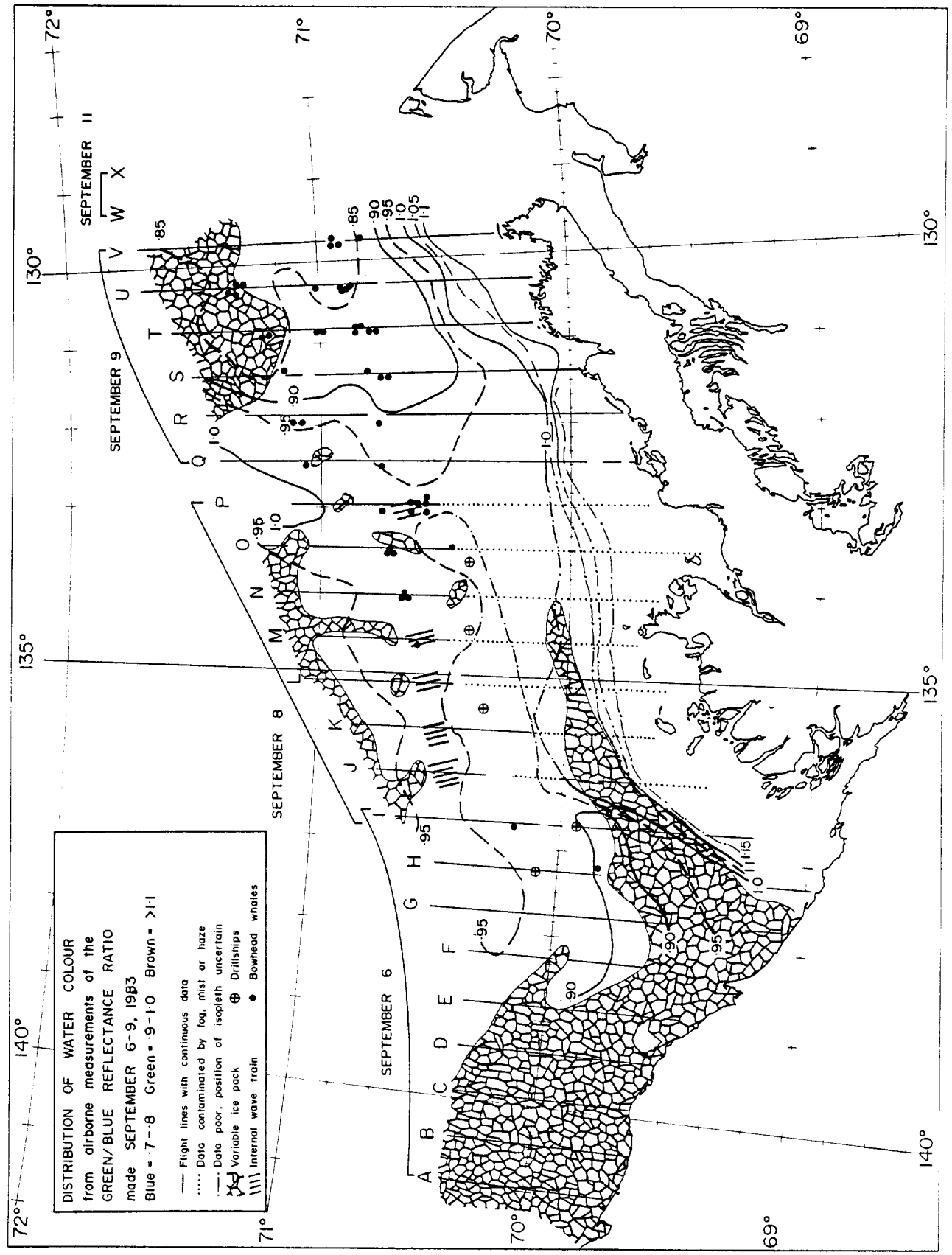

Fig. 24. Distribution of water colour in the Beaufort Sea 6-9 September 1983 as indicated by airborne measurements of the Green/Blue reflectance ratio (G/B).

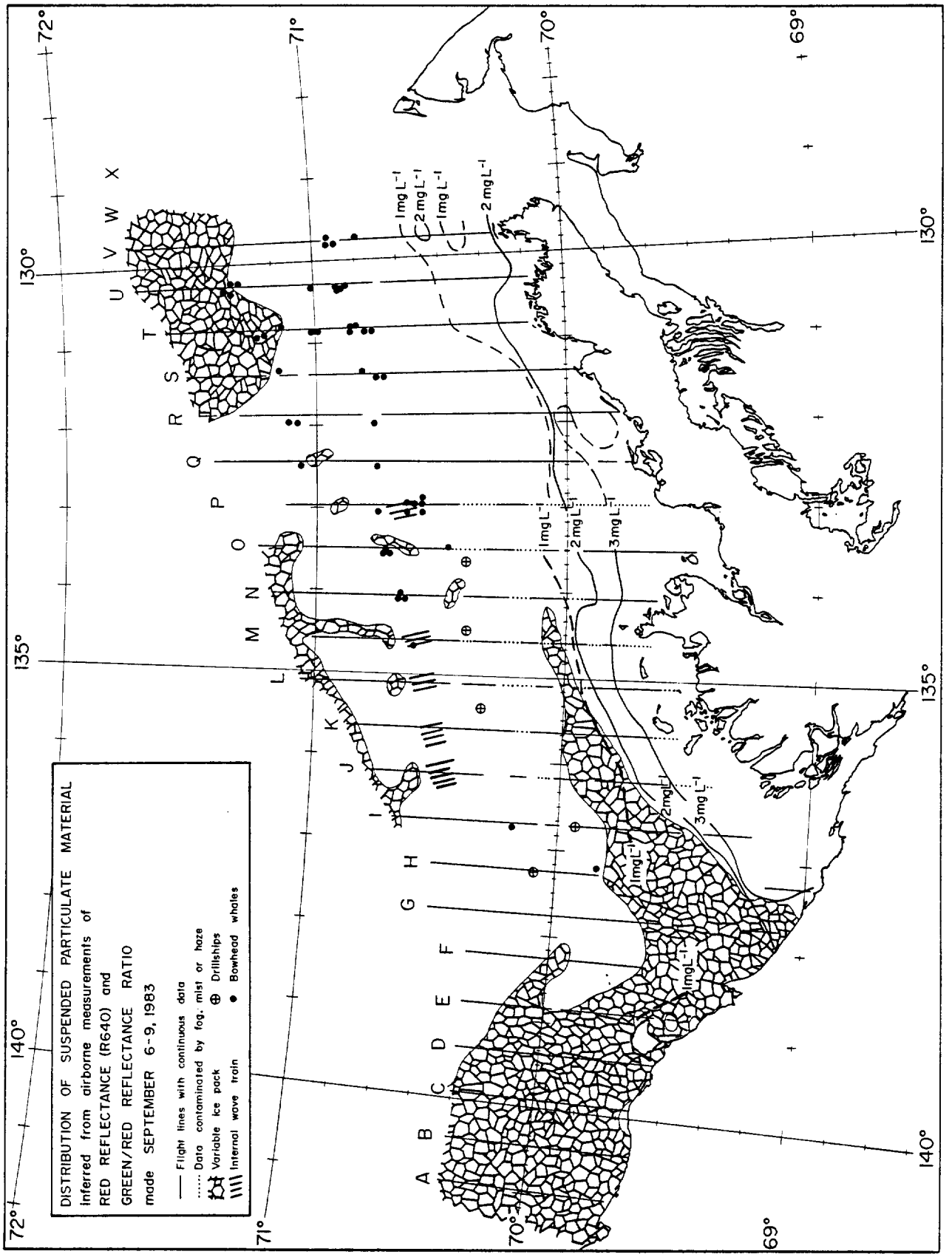

Fig. 25. Distribution of Suspended Particulate Material (SPM) in the southern Beaufort Sea, 6-9 September 1983 as inferred from airborne Red Reflectance (R640) and the Green/Red reflectance ratio (G/R).

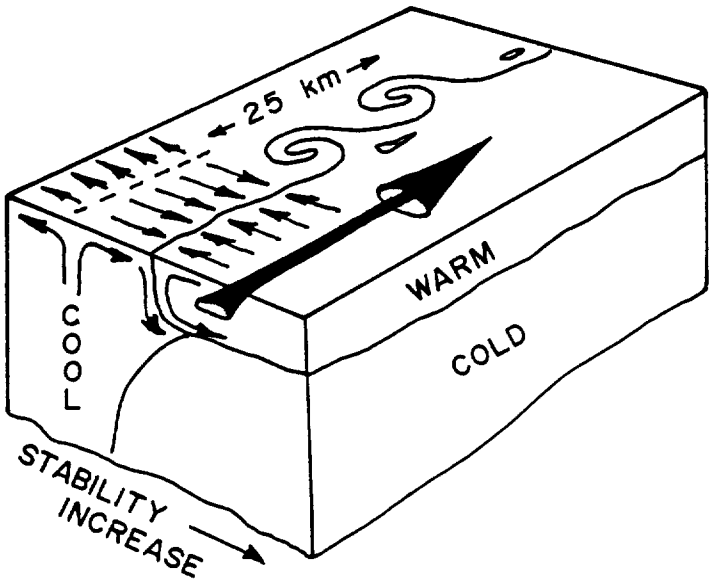

Fig. 31. Schematic diagram of frontal structure proposed by Simpson (1981), based on ship and satellite observations. The vertical circulation suggested is based on indirect evidence from temperature structure and observation of a surface convergence zone near the line of maximum surface temperature gradient.

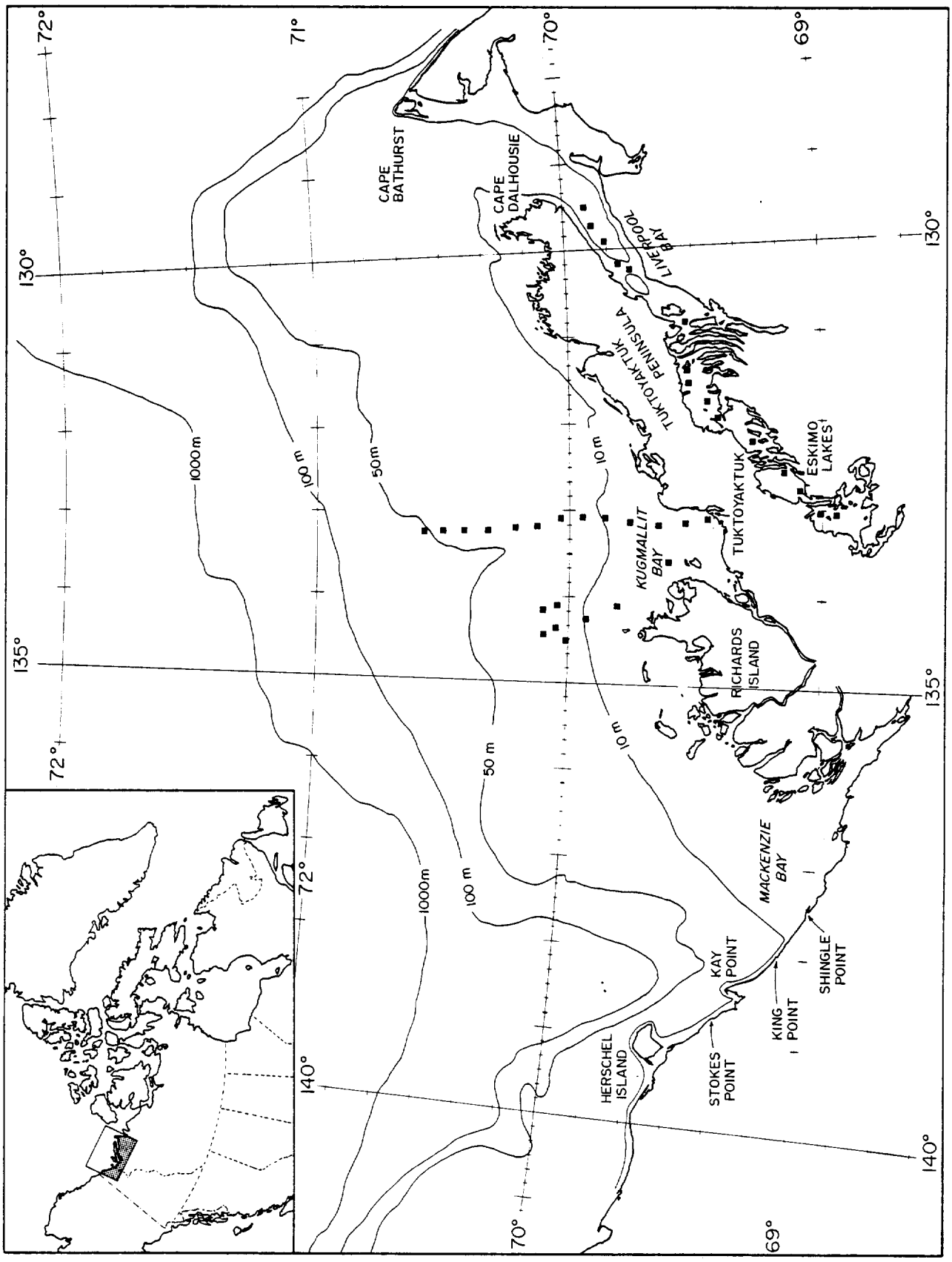

Fig. 32. The southern Beaufort Sea, showing place names used in the text, generalized bottom topography and calibration stations. Inset shows location of the Beaufort sea relative to northern Canada.

Plates

Plate 1

Top Left:

Sea surface thermal patterns in Mackenzie Bay 14 August 1983 (NOAA-7 AVHRR BAND 4). Approximate temperature range 2°C (blue) to 13°C (red). Land is black, cloud and ice are white. Patterns indicate strong surface flow past Herschel Island towards the northwest, probably resulting from easterly winds in preceding week. Upwelling west of the island is suggested by very low temperatures there.

Top Right:

Surface turbidity patterns in the southern Beaufort Sea 14 August 1983 (NOAA-7 AVHRR Band 1). Turbidity (suspended particulate load) increases from blue to red. Land is black, cloud and ice are white. Small amount of red near cloud at right is not turbidity.

Bottom Left:

Sea surface thermal patterns in the southern Beaufort Sea 12 September 1983 (NOAA-7 AVHRR Band 4). Coldest temperatures are blue, land is black, clouds and pack ice are white. White tongue through middle of image is ice.

Bottom Right:

Surface turbidity patterns in the southern Beaufort Sea, 12 September 1983 (NOAA-7 AVHRR Band 1). Turbidity (suspended particulate load) increases from blue to red. Land is black, cloud and ice are white.

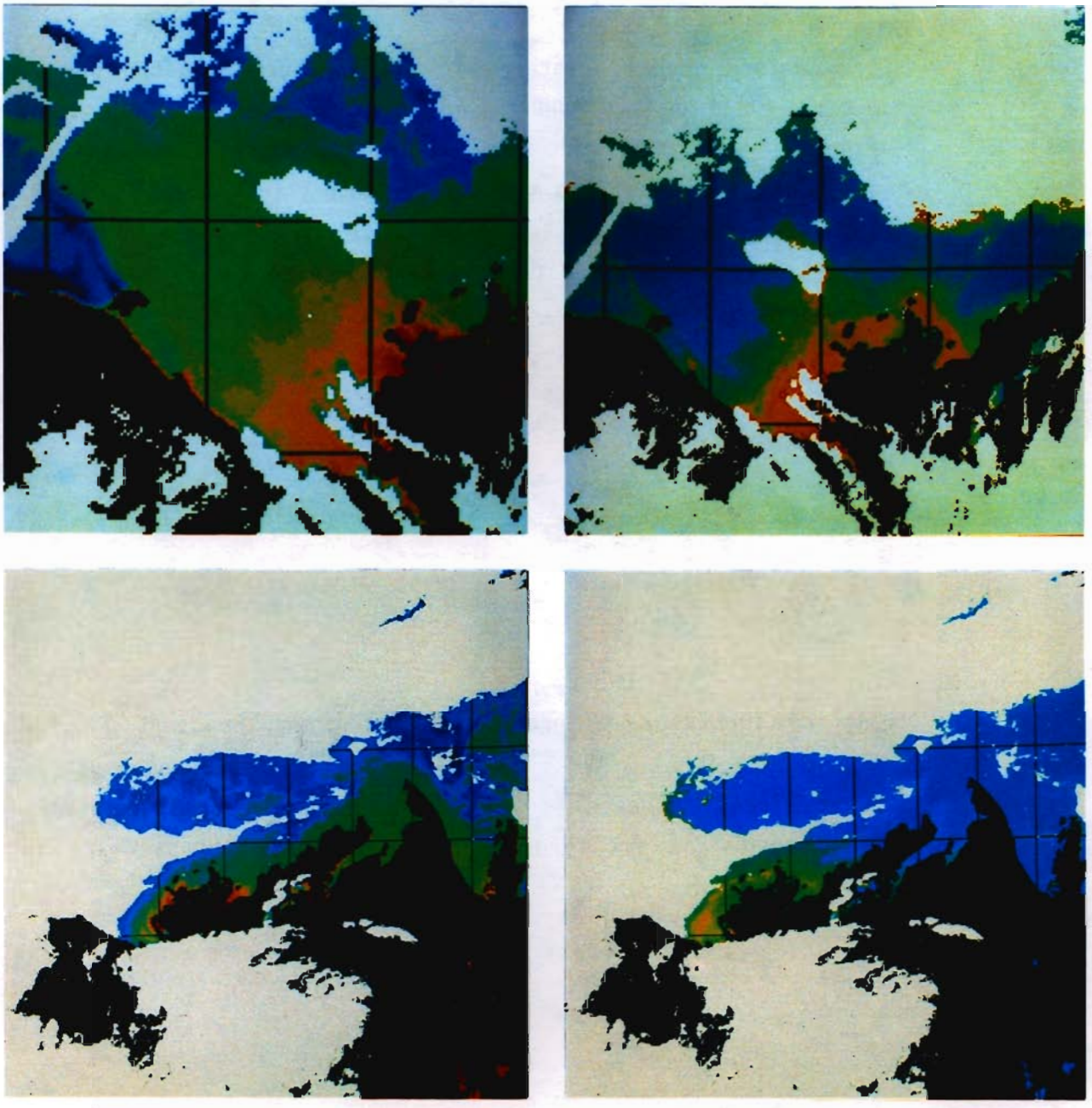

Plate 2

Top: Sea surface thermal patterns in the southern Beaufort Sea 22 August 1983 (NOAA-7 AVHRR Band 4). Approximate temperature range 2°C (blue) to 14°C (red). Land is black, cloud and ice are white. Black north-south lines are flight tracks of 1983 bowhead whale survey. Red squares are single whale sightings reported by McLaren and Davis (1984). Large square represents 25 whales.

Bottom: Surface turbidity patterns in the southern Beaufort Sea 22 August 1983 (NOAA-7 AVHRR Band 1). Turbidity (suspended particulate load) increases from blue to orange. Land is black, cloud over land and through centre of image and pack ice in north are white.

Plate 3

Top: Sea surface thermal patterns north of Richards Island 22 August 1983. Same data as Plate 2 but with partial atmospheric correction, to show cold (blue) patch in upper left part of image. Obvious separation of warm (red-orange) plumes origninating in Kugmallit Bay and Mackenzie Bay may continue offshore with cold water between them.

Middle: Sea surface thermal patterns north of Capes Dalhousie and Bathurst 22 August 1983. Same data as Plate 2 to show details of bowhead whale distribution observed August 23 (two lines at left) and August 24. Very cold (blue) water northwest of Cape Bathurst is a result of turbulence caused by southeasterly winds.

Bottom: Sea surface thermal patterns in Mackenzie Bay 22 August 1983. Same data as Plate 2 to show details of whale distribution. First 3 lines at left were flown August 19, next 4 on same day as image. Small squares represent single animals, large square represents 25 whales observed along the transect shown. Other observations indicate nearly 200 bowheads were distributed through the cold (blue) waters near the Yukon coast (McLaren and Davis 1984). High chlorophyll fluorescence and cold surface temperatures (near 2-3°C) suggest this water was the result of local upwelling.

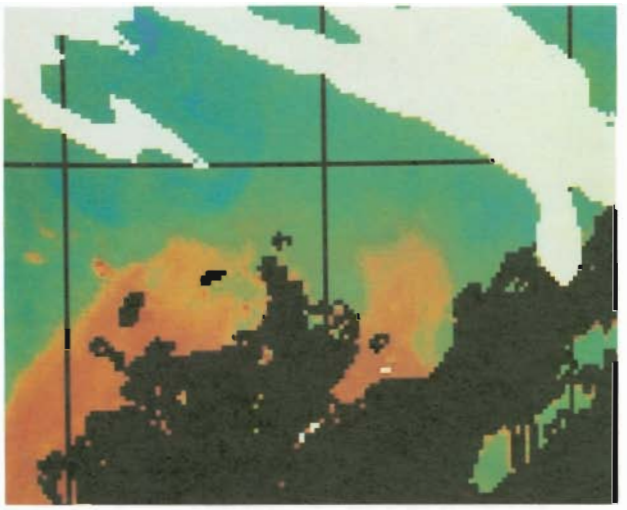

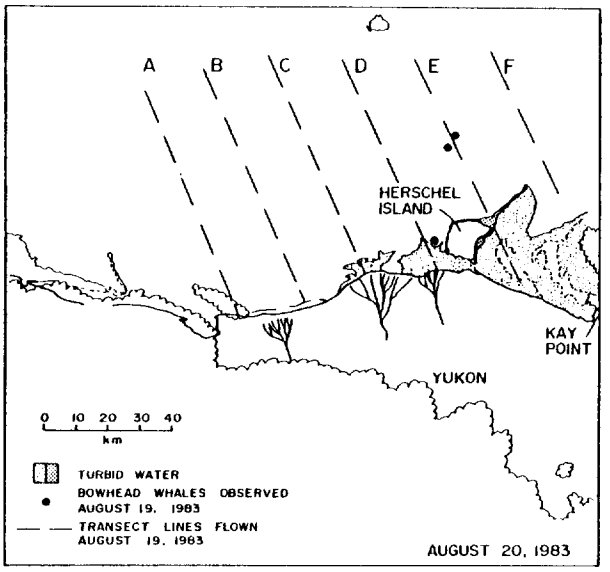

Fig. 18a. and Plate 4 Top: Sketch map to show main features visible in the LANDSAT MSS Band 2 image, 20 August 1983 (Plate 4 top). Turbidity trail extending from Herschel Island indicates net surface flow towards the east. Internal oscillations resulting from a switch from easterly to southwesterly winds on 18 August may be responsible for the zig-zag pattern.

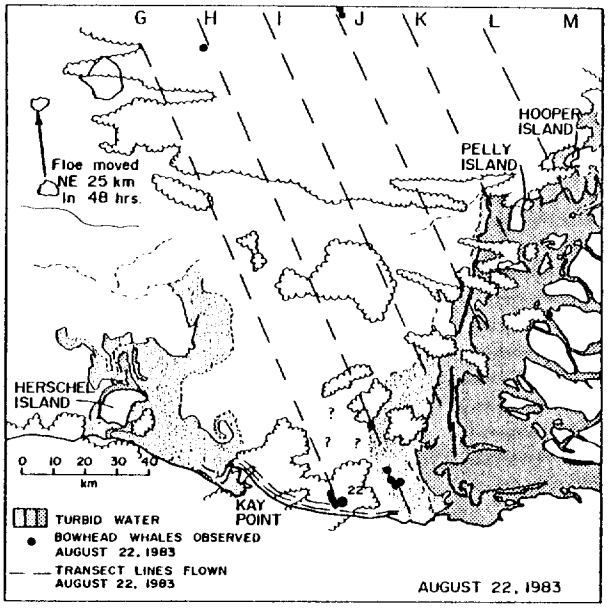

Fig. 18b. and Plate 4 Bottom: Sketch map to show main features of LANDSAT MSS Band 2, 22 August 1983 (Plate 4 bottom). Turbidity patterns near Herschel Island and ice drift indicate net northward surface drift. Position of east-west linear feature at centre left of image coincides with the position of the thermal discontinuity separating cold turbid waters near Herschel Island from warmer waters further north.

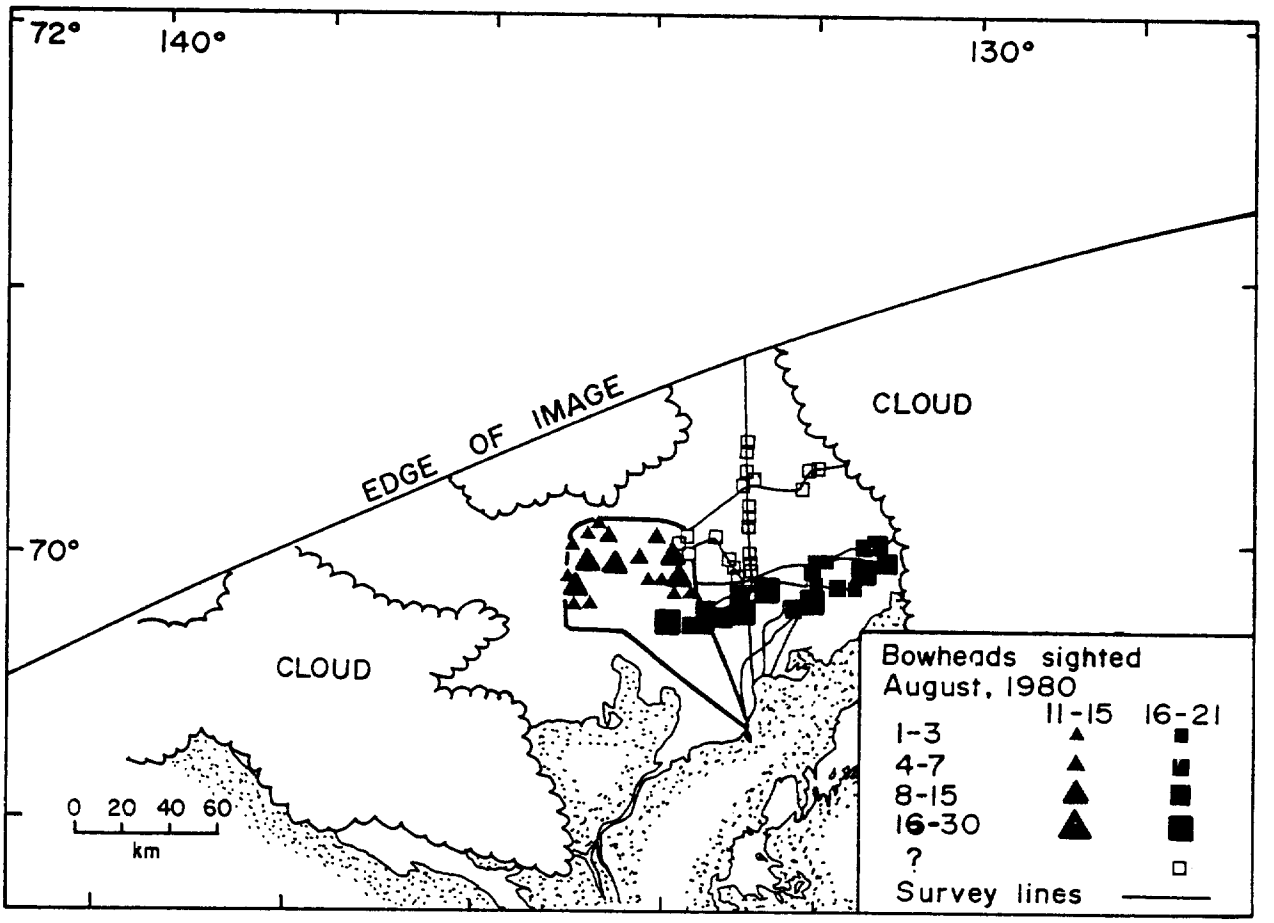

Fig. 26. Distribution of bowhead whale sightings 11-21 August 1980 in the area covered by satellite imagery in Plate 5. Redrafted from Richardson (1983). Flight lines are not shown in the area surveyed extensively 11-15 August.

Plate 5

Top: Sea surface thermal patterns north of Kugmallit Bay 20 August 1980 (NIMBUS-7 CZCS Band 6). Large numbers of bowhead whales are concentrated along a band of cool (blue) water just at the edge of the sediment plume (see below). Survey coverage and symbols are for 16-21 August only.

Bottom: Surface turbidity patterns north of Kugmallit Bay 20 August 1980 (NIMBUS-7 CZCS Band 3). Large numbers of bowheads are concentrated within a few km of the outer edge of the turbid water. The eddies and turbelence evident along the plume edge at left continued throughout the area in which whales were observed. Survey coverage and symbols explained above.

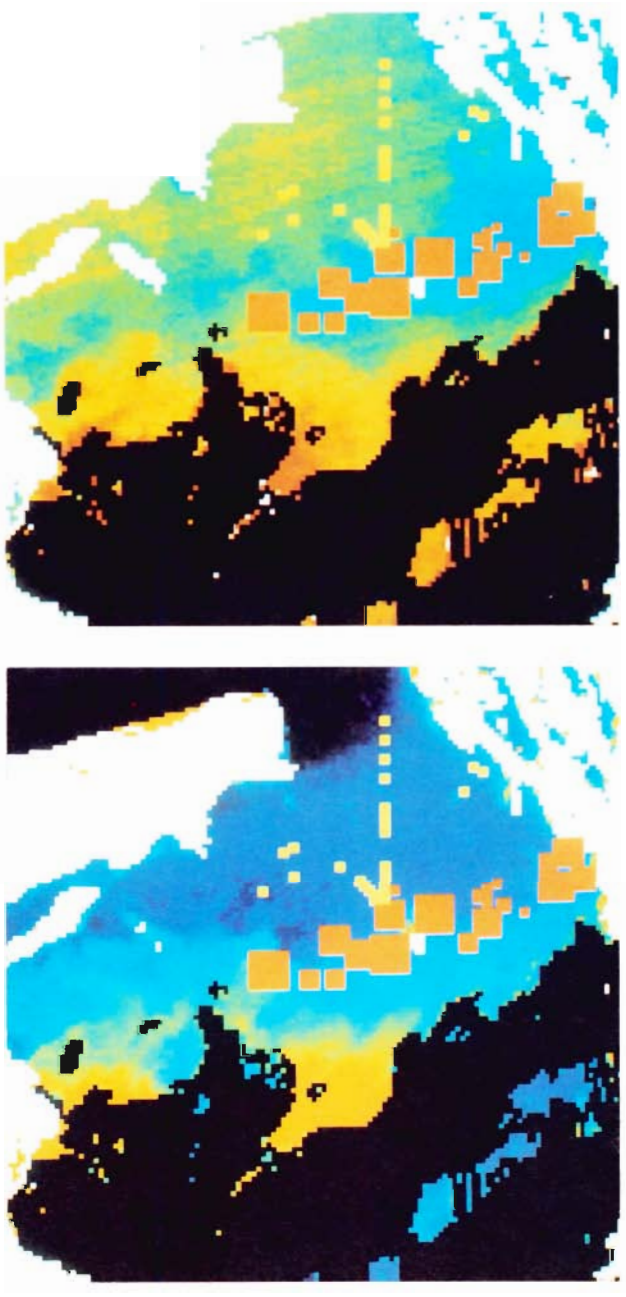

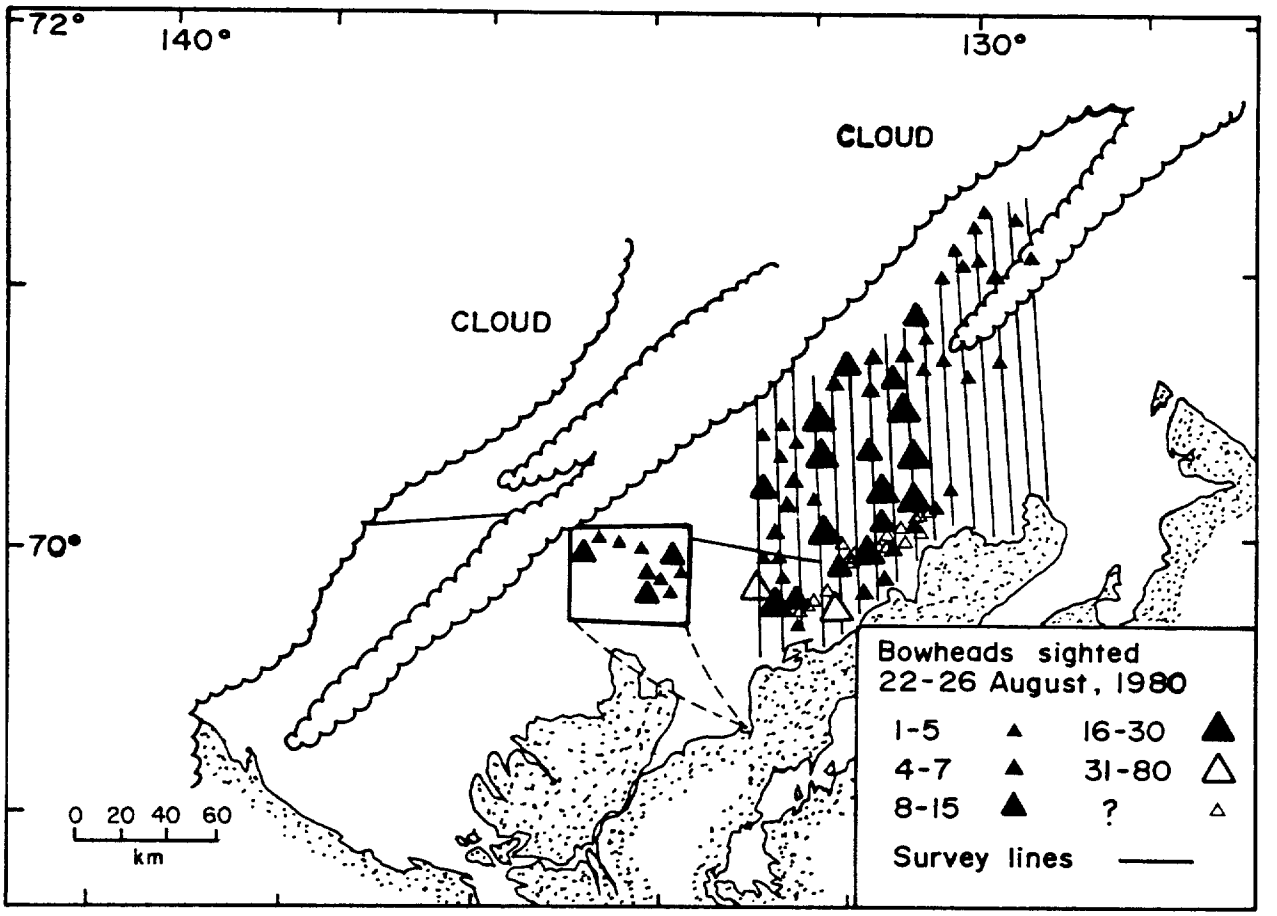

Fig. 27. Distribution of bowhead whale sightings 21-24 August 1980 in the area covered by the satellite images in Plate 6. Flight lines are not shown for small area north of Richards Island which was surveyed intensively. Redrafted from Richardson (1983).

Plate 6

Top: Sea surface thermal patterns in the southern Beaufort Sea 24 August 1980 (NOAA-6 AVHRR Band 4). Large numbers of bowhead whales were observed near the eastern edge of the thermal plume originating in the Mackenzie River. Very cold water just north of Cape Bathurst indicates local upwelling as a result of southeasterly winds at this time.

Middle: Sea surface thermal patterns north of Kugmallit Bay, 24 August 1980. Same data as above, to show details of whale distribution relative to temperature structure. Animals north of Richards Island (at left) appear to be oriented along a linear cool feature probably remaining from cold band seen in Plate 5 (top) along the edge of the turbidity plume. Large groups were also seen on either side of a warm tongue issuing from Kugmallit Bay.

Bottom: Sea surface thermal patterns north of Cape Dalhousie, 24 August 1980. Same data as above to show details of bowhead distribution around the edge of the thermal plume originating in the Mackenzie River.

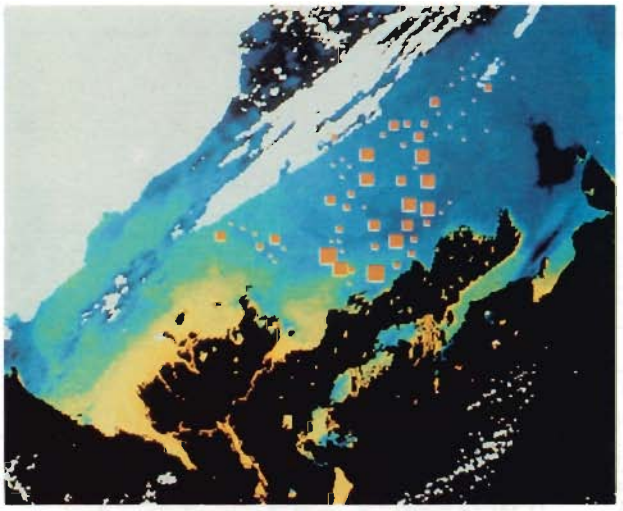

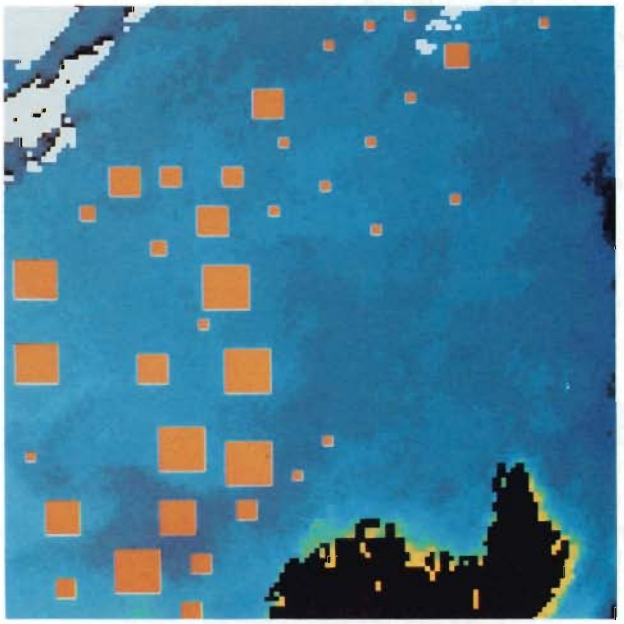

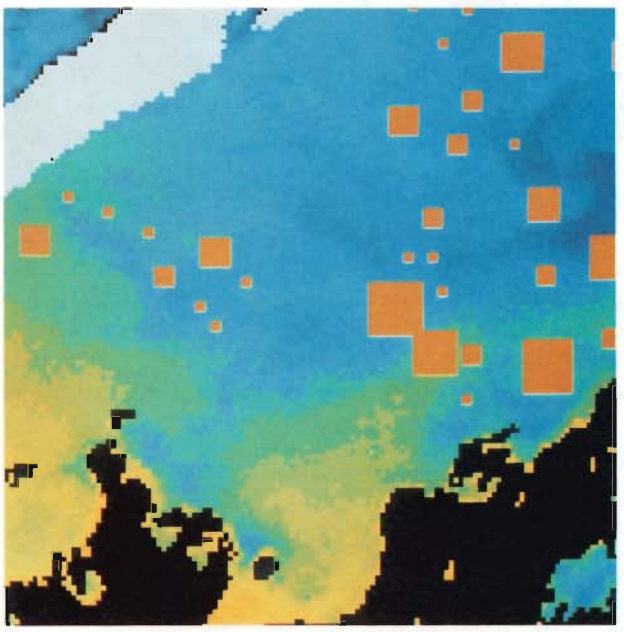

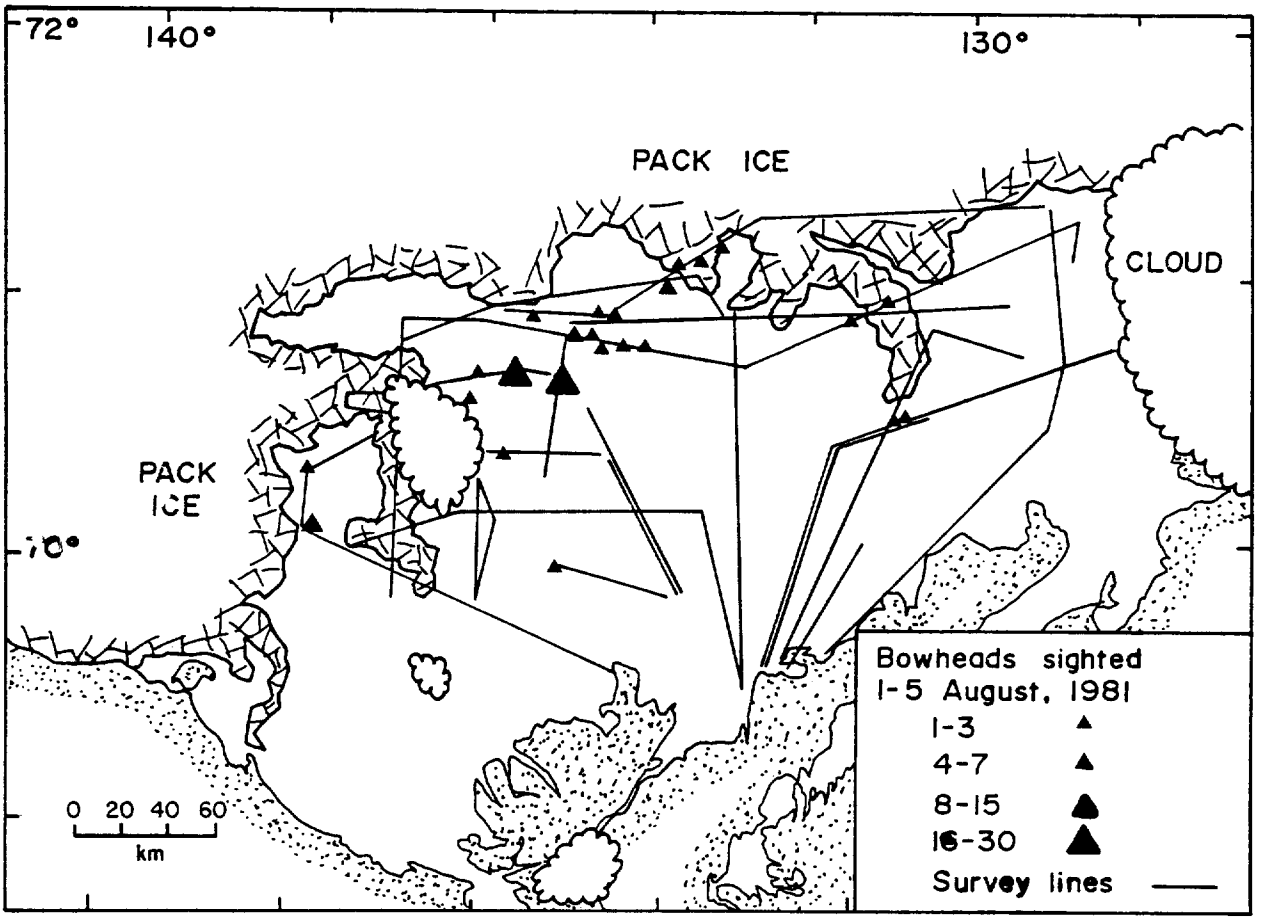

Fig. 28. Distribution of bowhead whale sightings 1-5 August 1981 during non-systematic observations summarized by Richardson (1983).

Plate 7

Top: Sea surface thermal patterns in the southern Beaufort Sea 5 August 1981 (NOAA-7 AVHRR Band 4). Small numbers of bowheads were observed near pack ice in the west and north.

Middle: Surface turbidity patterns in the southern Beaufort Sea 5 August 1981 (NOAA-7 AVHRR Band 1).

Bottom: Sea surface thermal patterns north of Richards Island 5 August 1981. Same data as above to show details of whale distribution and temperature. The largest groups were observed in a cold region of relatively weak thermal contrast.

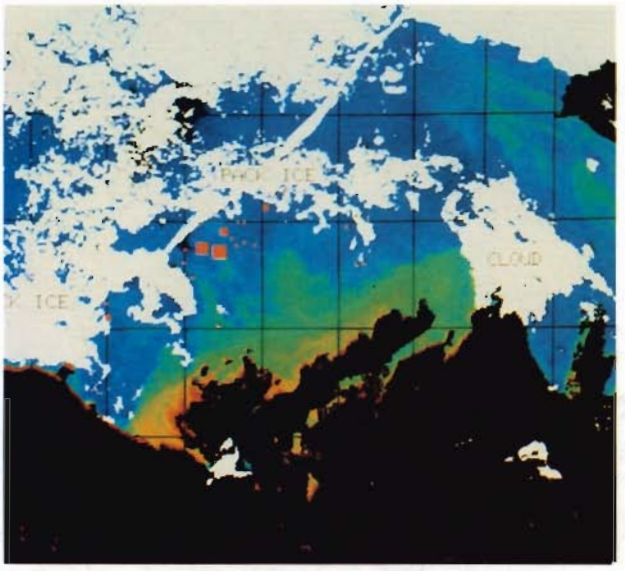
CLOUD

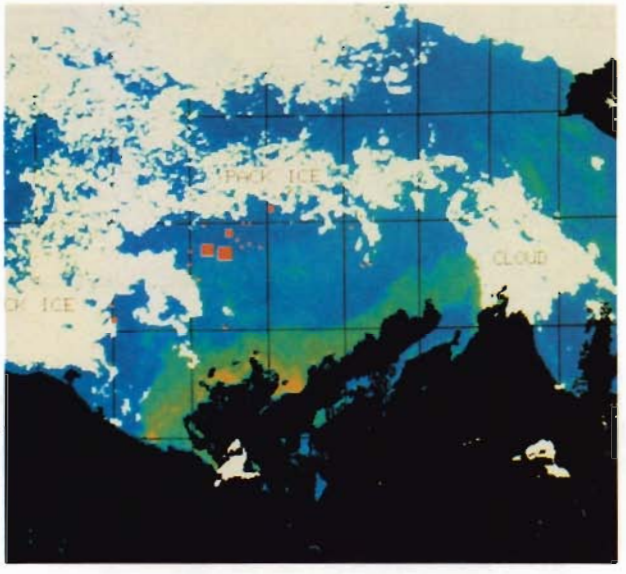
CLOUD

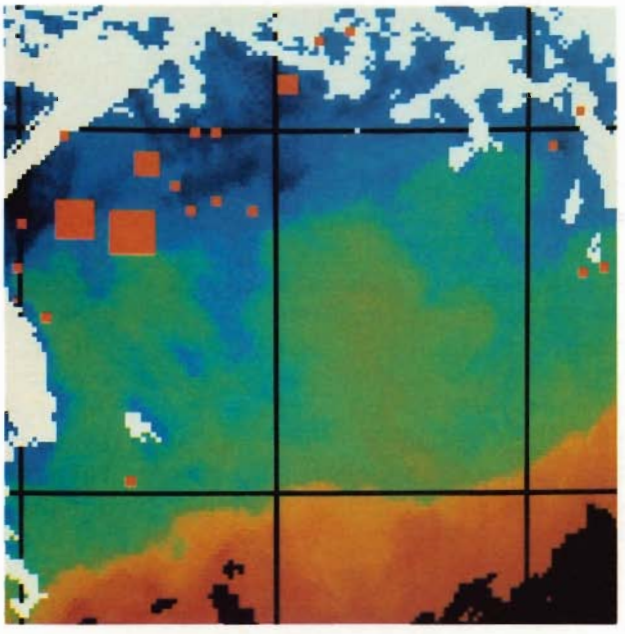

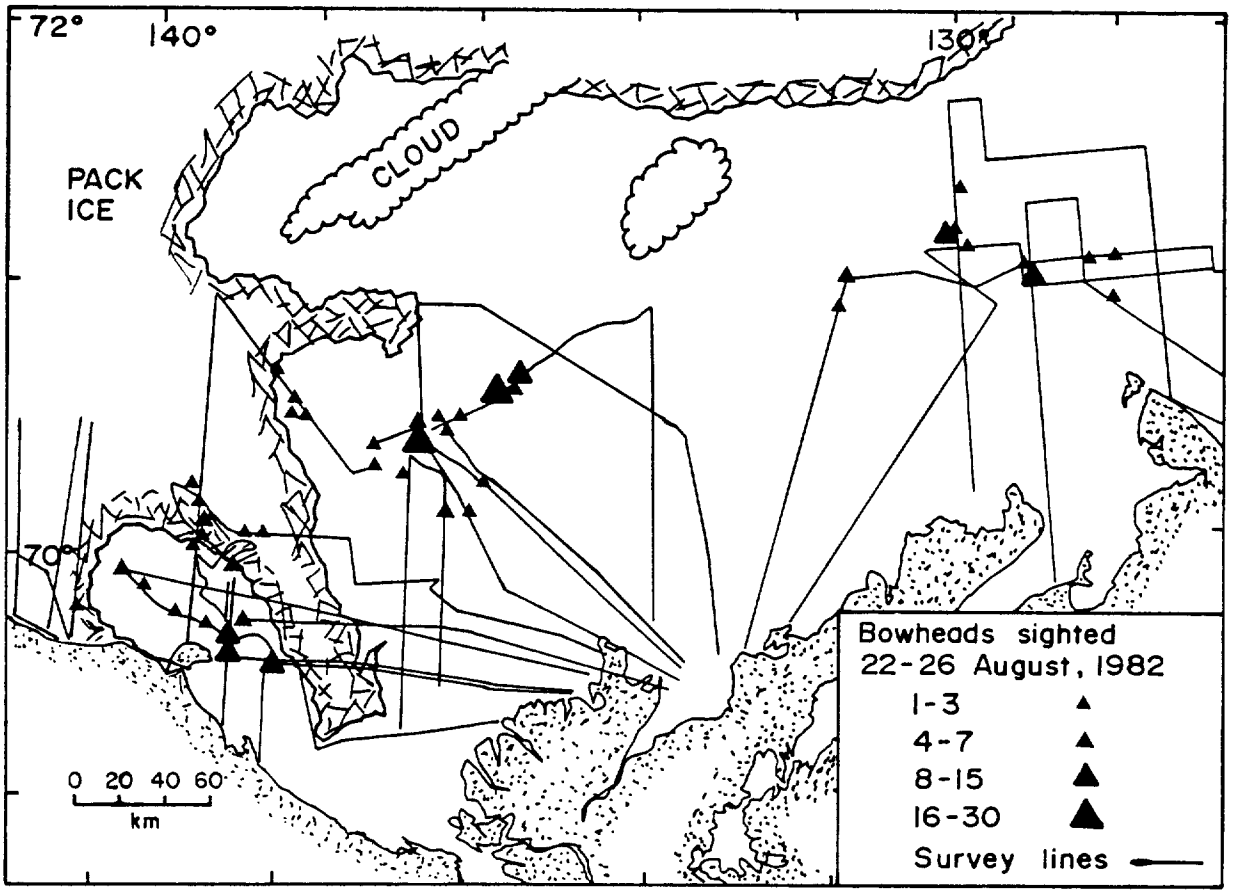

Fig. 29. Distribution of bowhead whale sightings 22-26 August 1982 during non-systematic observations summarized by Richardson (1983).

Plate 8

Top Left: Sea surface thermal patterns in the southern Beaufort Sea 26 August 1982 (NOAA-7 AVHRR Band 4). Linear white feature in upper left and circular feature at centre are jet aircraft contrails.

Top Right: Surface turbidity patterns in the southern Beaufort Sea 26 August 1982 (NOAA-7 AVHRR Band 1). Note differences between thermal and turbidity plumes.

Bottom Left: Sea surface thermal patterns northwest of Richards Island to show details of bowhead distribution relative to confused thermal structure visible north of 70°N.

Bottom Right: Sea surface thermal patterns north of Capes Dalhousie and Bathurst. Small numbers of animals were located along the outer edge of the thermal plume originating in the Mackenzie River. Note the sharp thermal structure near Cape Bathurst.

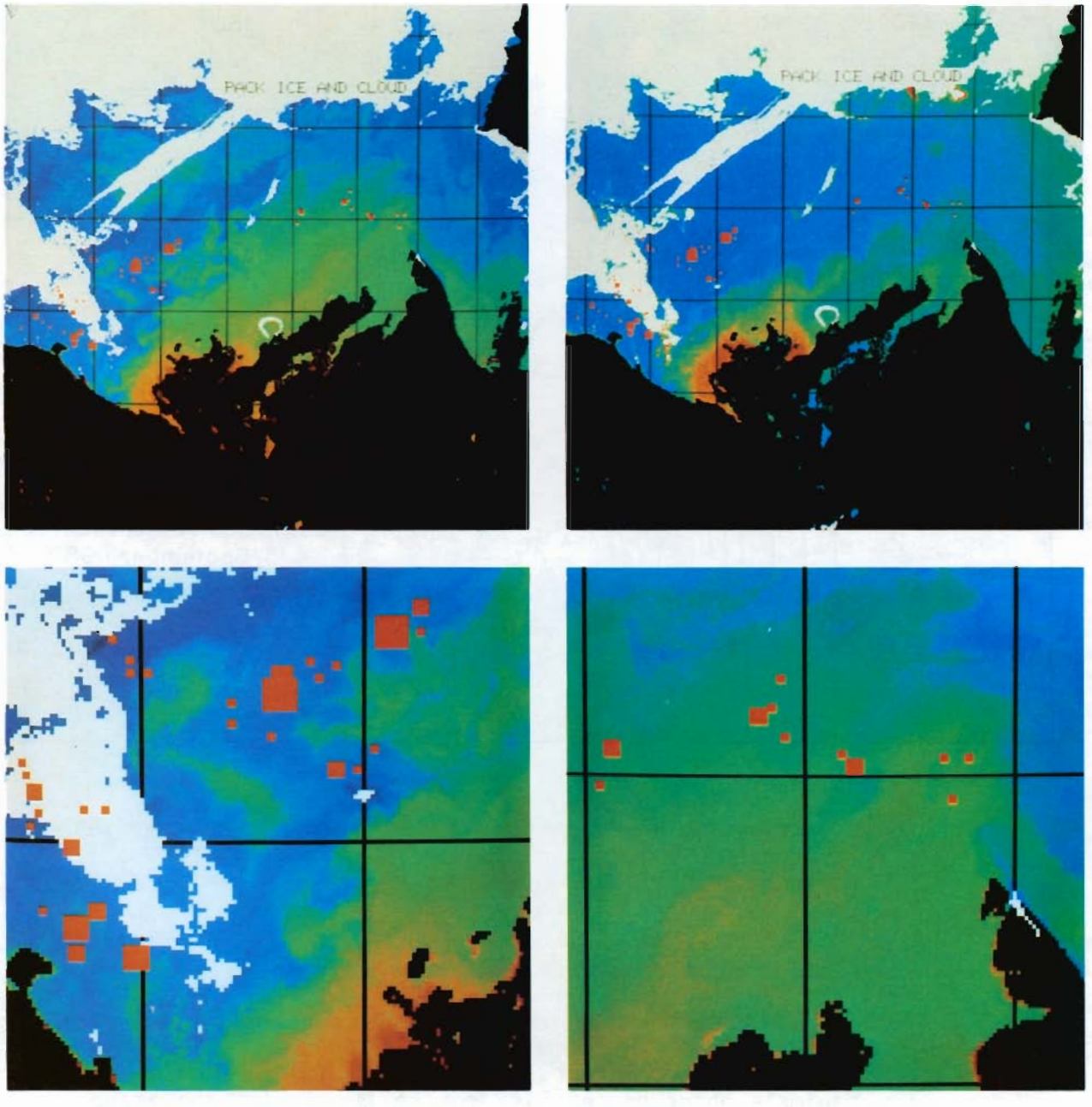
PACK ICE AND CLOUD
PACK ICE AND CLOUD

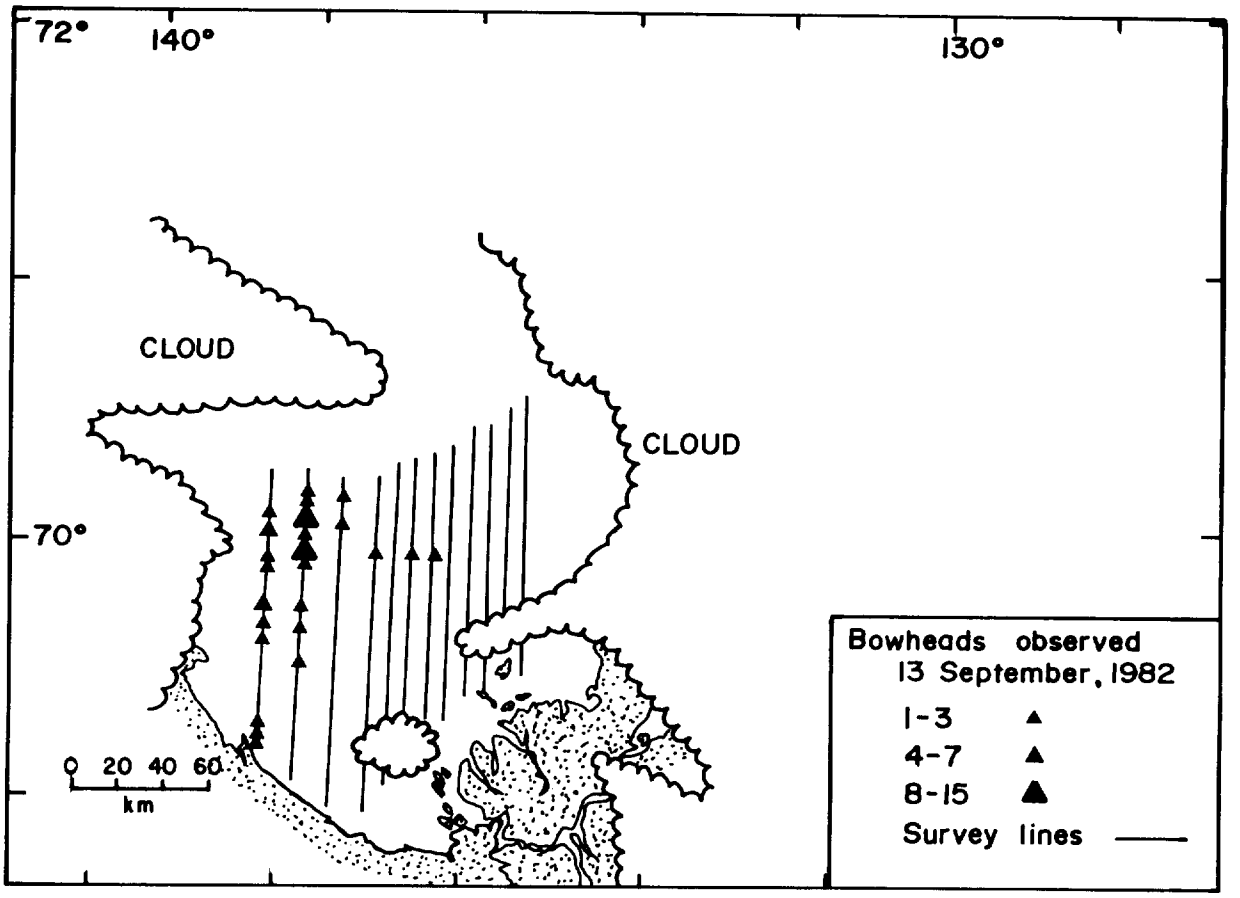

Fig. 30. Distribution of bowhead whale sightings 13 September 1982 on systematic surveys in the area covered by the satellite imagery in Plate 9. Redrafted from Richardson (1983).

Plate 9

Top: Sea surface thermal patterns in Mackenzie Bay 13 September 1982 (NOAA-7 AVHRR Band 4). A few bowheads were seen near a strong thermal front just off Kay Point, but nearly all animals observed in this area on the day of the image were congregated near thermal discontinuities further north (70°N, 138°W).

Bottom: Surface turbidity patterns in Mackenzie Bay 13 September 1982 (NOAA-7 AVHRR Band 1). Patterns away from the river delta are only poorly defined in the visible spectrum.

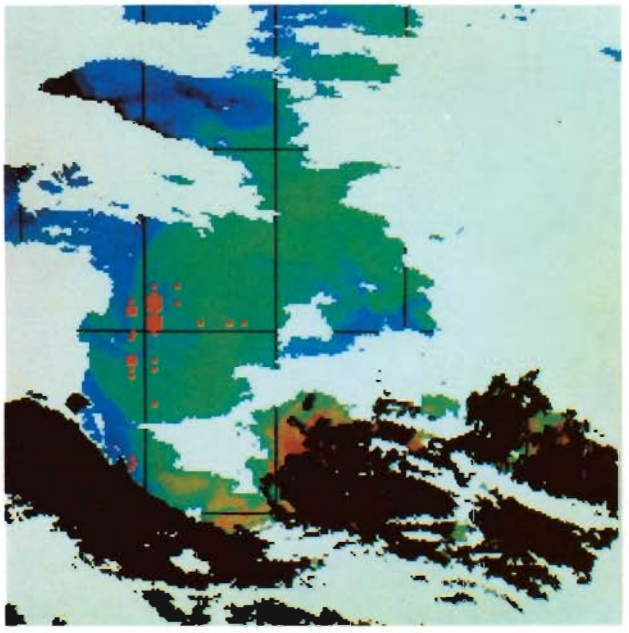

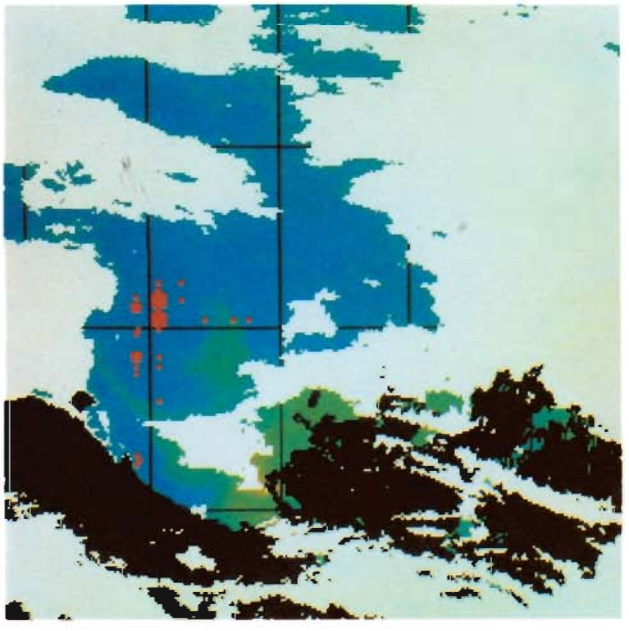

APPENDICES

APPENDIX 1. LOGISTICAL SUMMARY (1983 SURVEYS)

August

15	Arrived Inuvik. Instrumentation tested. Test data sent south for processing.
19	Arrived Tuktoyaktuk. Line A, B, C, D, E, F (09:44 - 14:10 h). Heavy overcast over this area, incident signals were very low. Some rain and snow, haze. Data were very noisy. Interference (ground loops) between instruments confirmed so PRT-5 and strip-chart recorder disconnected.
20	Lines O, P, Q (08:30 - 11:50 h). Heavy overcast near shore, clear offshore or high stratus over Line O. Fog and mist on south half of lines P and Q.
21	Calibration exercise with helicopter in area of Pullen Island (10 stations with surface samples)(14:40 - 17:30 h)
22	Two lines parallel the Yukon coast and G, H, I, J, K, L (09:30 - 17:00 h). Skies clear or thin stratus. Data were good.
23	Lines M, N, R, S (08:50 - 14:00 h). Heavy overcast, intermittent rain in south; broken light status offshore and on line N, R. Some clear skies on line S. Signals very low and noisy on southern half line M. Strong absorption lines. Calibration exercise with helicopter. Line of 13 samples north of Tuktoyaktuk to 70°40'N (16:00 - 18:20 h).
24	Lines T, U, V, W (08:20 - 18:20 h). haze, mist on most of these lines.

September

5	Instrument tested at Inuvik. Flew to Tuktoyaktuk.
6	Lines A, B, C, D, E, F, G, H, I (09:38 h - 17:25 h). Overcast along A, B, C sky; clear near south half of D, E, F and on lines G, H, I. A, B, C, D and south half of E, F, G, H covered by 0.4 - 0.8 open pack, Very few data obtained because of ice.
7	Too windy for whale survey.
8	Lines I, J, K, L, M, N, O, P (08:50 h - 18:30 h). Heavy overcast except near offshore ends of lines. Fog and mist was over southern half of all these lines J, K, M, N and O.
9	Lines Q, R, S, T, U, V (08:30 h - 15:30 h). Sunny and clear for Q and R but low sun angle caused very low incident signals (=noisy data). Less noise later in morning as sun rose. Some high stratus and haze occurred along lines S, T.
10	Fog - no flight.
11	Lines W, X (13:20 h - 15:50 h). Cloudy, low ceiling, fog, most, snow. Winds of 25-30 knots, whitecaps and spray everywhere. Reflectance data were not processed.

APPENDIX 2. METEOROLOGICAL SUMMARY (1983 SURVEYS)

August

15-17	High pressure cell near Banks Island, near low on Yukon Coast. High moved west, then south. Winds at drillships easterly 20 knots, decreasing to west 5 knots by the 17 August.
18	High pressure centre over drillships, moved east very quickly. Strong low north of Alaska and warm front along Alaska coast. Winds at drillships southerly 15 knots, 12Z-2400Z on 18 August.
19	Trough moved through on 19 August near 1800Z, winds westerly but swinging.
20	Low off Alaska; trough along Yukon Coast; winds at drillships confused.
21-22	Winds southwesterly 15-25 knots.
23-25	Winds easterly and southwesterly until 24 August. Front moved through on 23 August; winds switched to northwesterly 10-20 knots.
26	High pressure cell moved across delta region - 0600Z.
27	Winds south and southwesterly at drillships.

September

5	Southerly 20 knots then northwesterly 25 kn after passage of cold front.
6	High pressure cell moved over delta, winds westerly 10-15 knots.
7	Deep low moved along Alaska Coast, winds southerly 10-35 knots.
8	Low passed late on 7 September, winds westerly 5-10 knots.
9	Weak high pressure ridge over southern Beaufort, winds southwesterly 5-15 knots.
10	Warm front passed late on 9 September, winds westerly 10-20 knots, cold front passed late on 10 September.
11	Winds easterly 5-15 knots.

APPENDIX 3. CALIBRATION DATA

21 August 1983

Station	Position		Temperature	Salinity	Secchi	Munsell Colour	Chl + Ph	(% Chl)	SPM
1	70° 05' N,	134° 31' W	8.1	14.99	5		0.12	(83)	< 0.1
2	70° 06' N,	134° 31' W	7.9	14.34	5		0.15	(73)	0.8
3	70° 04' N,	134° 25' W	8.9	23.82	6	10 GY	0.17	(59)	< 0.1
4	70° 06' N,	134° 27' W	8.5	15.14	7	5G/5GY	0.16	(75)	0.5
5	70° 04' N,	134° 21' W	9.6	25.06	7	5 G	0.14	(71)	3.3
6	70° 05' N,	134° 10' W	9.3	21.64	7	5 G	0.10	(66)	2.4
7	70° 04' N,	134° 05' W	9.0	24.33	4.5	5 G	0.21	(67)	4.4
8	69° 56' N,	134° 17' W	9.2	22.77	3.5	5 G	0.38	(47)	2.7
9	69° 47' N,	134° 07' W	9.3	22.23	1.5	10 GY	0.13	(65)	4.1
10	69° 36' N,	133° 37' W	11.5	9.01	< 0.5	5 Y	0.78	(74)	17.9

23 August 1983

Station	Position		Temper-ature	Salinity	Secchi	Munsell Colour	Chl + Ph	(% Chl)	SPM	G/B	G/R	R640
1	70° 33' N,	133° 14' W	9.3	20.88	8	5 G	0.04	(43)	-	0.86	4.2	0.010
2	70° 30' N,	133° 13' W	8.5	22.11	8	10 GY	0.11	(46)	< 0.1	0.84	4.5	0.011
3	70° 25' N,	133° 13' W	9.6	23.20	7	10 GY	0.10	(56)	0.8	0.85	4.6	0.005
4	70° 20' N,	133° 12' W	10.0	23.87	6	5 G	0.10	(47)	-	0.85	4.8	0.007
5	70° 13' N,	133° 11' W	10.0	24.69	5	5 G	0.13	(55)	0.8	0.88	4.8	0.008
6	70° 08' N,	133° 09' W	9.9	26.08	5	5 G	0.11	(60)	6.0	0.86	4.9	0.021
7	70° 03' N,	133° 05' W	10.0	25.05	4.5	5 G	0.15	(57)	-	0.89	5.1	0.010
8	69° 56' N,	133° 03' W	12.4	26.19	2	-	0.55	(51)	3.1	0.93	3.1	0.060
9	69° 54' N,	133° 03' W	12.9	10.69	1.5	5 GY	0.74	(61)	-	1.07	2.0	0.085
10	69° 46' N,	133° 09' W	13.6	6.58	1.0	10 Y	0.56	(77)	9.45	0.97	1.8	0.165
11	69° 39' N,	133° 10' W	14.4	5.24	0.5	-	0.76	(72)	13.35	1.1	1.3	0.185
12	69° 34' N,	133° 08' W	13.2	8.38	1	5 GY	1.0	(54)	-	1.06	2.1	0.090
13	69° 27' N,	133° 04' W	13.8	13.11	1	5 G	0.66	(56)	-	1.04	3.2	0.060
14	69° 27' N,	133° 03' W	11.5	21.10	2	5 G	1.2	(55)	-	1.07	3.7	0.074

9 October 1983

Station	Position		Salinity	Chl + Ph (% Chl)		SPM	G/B	G/R	R640
1	68° 58' N,	133° 10' W	3.32	0.64	(81)	1.95	-	-	-
2	69° 00' N,	133° 04' W	3.31	0.56	(82)	2.74	0.95	3.1	0.088
3	69° 06' N,	132° 46' W	8.00	0.42	(73)	4.31	0.95	2.7	0.086
4	69° 09' N,	132° 33' N	7.99	0.37	(76)	3.53	0.98	2.8	0.101
5	69° 16' N,	132° 16' W	12.53	0.24	(71)	3.10	0.92	3.2	0.100
6	69° 24' N,	131° 57' W	14.17	0.18	(67)	2.21	0.92	3.5	0.042
7	69° 27' N,	131° 48' W	15.01	0.31	(65)	1.44	0.91	3.4	0.044
8	69° 30' N,	131° 33' W	15.26	0.33	(67)	1.97	0.89	3.4	0.035
9	69° 33' N,	131° 23' W	16.42	0.40	(63)	2.04	0.92	3.1	0.035
10	69° 32' N,	130° 55' W	17.72	0.48	(60)	3.07	0.91	2.8	0.039
11	69° 45' N,	130° 14' W	22.60	0.90	(54)	13.70	1.04	1.5	0.125
12	69° 48' N,	130° 10' W	22.21	0.75	(52)	11.30	1.03	1.6	0.148
13	69° 51' N,	129° 53' W	21.58	0.93	(57)	8.44	1.0	1.8	0.169
14	69° 54' N,	129° 42' W	21.00	0.60	(67)	4.57	0.98	2.6	0.084
15	69° 55' N,	129° 27' W	20.87	0.48	(73)	2.57	0.98	3.0	0.046

APPENDIX 4. FILTER SONIFICATION EXPERIMENT

Filter Number	Wt of Sediment on Filter (mg)	Wt Loss After Sonification (mg)	% Removal
1	0.5	0.55	110
2	0.59	0.72	122
3	0.17	0.37	217
4	0.35	0.32	91
5	1.05	1.15	110
6	2.40	2.65	110
7	3.34	3.25	98
8	4.03	3.92	97
9	4.42	4.50	102
10	4.51	4.46	99
11	8.52	6.63	78
12	8.62	7.78	90
13	9.43	8.60	91
14	10.94	10.63	97
15	10.32	10.19	99
16	12.54	11.50	92
Control 1	0	0.14	
Control 2	0	0.04	
Control 3	0	0.51 (gain)	

Weighing error for blank filters (n=12) 15.58 ± 0.12 mg % SD=0.8